arXiv:1511.04230v2 [math-ph] 30 Nov 2015

Relation between two-phase quantum walks and the topological invariant

Takako Endo[a]

Department of Physics, Ochanomizu University
2-1-1 Ohtsuka, Bunkyo, Tokyo, 112-0012, Japan

LERMA, Observatoire de Paris, PSL Research University, CNRS, Sorbonne Universités, UPMC Univ. Paris 6, UMR 8112, F-75014
4 place Jussieu 75005 Paris, France

Norio Konno[b]

Department of Applied Mathematics, Faculty of Engineering, Yokohama National University
79-5 Tokiwadai, Hodogaya, Yokohama, 240-8501, Japan

Hideaki Obuse[c]

Department of Applied Physics, Hokkaido University
Kita 13, Nishi 8, Kita-ku, Sapporo Hokkaido 060-8628, Japan

Abstract

We study a position-dependent discrete-time quantum walk (QW) in one dimension, whose time-evolution operator is built up from two coin operators which are distinguished by phase factors from $x \geq 0$ and $x \leq -1$. We call the QW the *complete two-phase QW* to discern from the two-phase QW with one defect[13, 14]. Because of its localization properties, the two-phase QWs can be considered as an ideal mathematical model of topological insulators which are novel quantum states of matter characterized by topological invariants. Employing the complete two-phase QW, we present the stationary measure, and two kinds of limit theorems concerning *localization* and the *ballistic spreading*, which are the characteristic behaviors in the long-time limit of discrete-time QWs in one dimension. As a consequence, we obtain the mathematical expression of the whole picture of the asymptotic behavior of the walker in the long-time limit. We also clarify relevant symmetries, which are essential for topological insulators, of the complete two-phase QW, and then derive the topological invariant. Having established both mathematical rigorous results and the topological invariant of the complete two-phase QW, we provide solid arguments to understand localization of QWs in term of topological invariant. Furthermore, by applying a concept of *topological protections*, we clarify that localization of the two-phase QW with one defect, studied in the previous work[13], can be related to localization of the complete two-phase QW under symmetry preserving perturbations.

Keywords: quantum walk, two-phase system, localization, weak limit measure, topological invariant

[a]endo.takako@ocha.ac.jp (e-mail of the corresponding author)
[b]konno@ynu.ac.jp
[c]hideaki.obuse@eng.hokudai.ac.jp

1 Introduction

Quantum walks (QWs) are considered as quantum counterparts of classical random walks. There are mainly two kinds of QWs, that is, the discrete-time QW and continuous-time one[21, 31]. In this paper, we focus on the discrete one. It was mathematically shown that quantum search algorithms constructed by QWs provide faster computations than the corresponding classical algorithms. As other applications, QWs are ideal platforms to study energy transportation efficiency of photosynthesis[34], and the Anderson localization in disordered systems[11, 40], for instance. Owing to the rich applications, it is of great importance to study the asymptotic behavior of QWs, however, it would be difficult to implement the states in the long-time limit by experiment. Moreover, because of its quantumness, it is difficult to understand QWs intuitively. Therefore, to understand the asymptotic behavior of QWs, it is exceedingly important both to numerically simulate the time-step evolution of QWs, and obtain limit theorems mathematically.

So far, two kinds of limit theorems have described the characteristic properties of QWs mathematically. The one is the limit theorem expressing localization. Localization is one of the typical properties of discrete-time QWs, which was first studied by Inui *et al.* [23] mathematically and numerically. The detailed definition of localization is devoted to [1, 24] for example. The other is the weak convergence theorem, which expresses ballistic spreadings of the walker by the weak limit measure, and is fully explained in [31], for instance. We should note that the weak limit measure is consisted by the Dirac measure part corresponding to localization and absolutely continuous part, corresponding to the ballistic spreading. The weak convergence theorem for space-homogeneous QWs in one dimension, such as Hadamard walk[29], Grover walk[9], was derived.

Nowadays, the research on the asymptotic behavior of space-inhomogeneous QWs is one of the hottest topics in the filed of QWs. Here we review the previous studies of inhomogeneous QWs briefly. Konno *et al.* [31] gave the weak convergence theorem for a one-dimensional QWs with one defect for the first time, taking advantage of the generating function of the weights of passages. Wojcik *et al.* [42] studied the other types of one-dimensional QWs with one defect, called the Wojcik model, and showed analytically and numerically that the Wojcik model exhibits astonishing localization effects for changing the phase of the defect. Then, Endo and Konno[15, 16] proved the prominent localization effect mathematically, and in subsequent, they gave the weak convergence theorem for the Wojcik model, which completed the whole description of the asymptotic behavior. Endo *et al.* [18] got a stationary measure of the QW with one defect whose quantum coin is defined by the Hadamard matrix at $x \neq 0$ and the rotation matrix at $x = 0$. Recently, Endo *et al.* [13, 14] studied the two-phase QW with one defect which has two different time-evolution operators in positive and negative spatial regions, in addition to another operator at the origin. They derived the limit theorems concerning localization and the ballistic behavior, and they clarified the effect of the two different quantum coins and initial coin state of the walker on the asymptotic behavior.

Recently, localization appearing in the space-inhomogeneous QWs has attracted attentions from a quite different direction, i.e., topological invariants characterized by eigenvectors of the QW[25, 27, 28]. This approach has emerged from recent developments on topological phases of matter in the condensed matter physics, known as topological insulators and superconductors[5, 10, 20, 37]. Since the QW can be considered as the simplified theoretical model of topological insulators (more preciously, Floquet topological insulators[26, 32]), the topological phase of quantum walks has been intensively studied[2, 3, 4, 7, 8, 12, 35, 36, 38, 41]. In the field of theoretical physics on the topological insulators, a fundamental principle, so-called the bulk-edge correspondence, predicts the existence of localized states at the interface where two adjacent spatial regions are characterized by different topological numbers. A recent work on the two-phase QW with one defect[13, 14] gives an opportunity to study localization of the space-inhomogeneous QW on the line in term of topological invariants. In the two-phase QW with one defect, however, there are three distinct spatial regions, i.e., positive, negative spatial regions and the origin. On the topological phase of matter, the topological invariant is generally defined for a system with a finite

spatial extent, roughly speaking, enough larger than the localization length of localized states. Thereby, the single defect at the origin may prevent to apply the argument of topological invariants straightforwardly.

In the present work, we study a complete two-phase QW which is defined by modifying the two-phase QW with one defect so that the coin operator at the origin is replaced with that in the positive space part. One of the important advantages to study the complete two-phase QW is that the model enables us to directly discuss the mathematically rigorous results on localization of the QW on the line in term of topological invariants.

First, we derive mathematically rigorous results on the stationary, time-averaged limit, and weak limit measures of the complete two-phase QW. There have been constructed several kinds of popular techniques to mathematically investigate the asymptotic behaviors of QWs, such as the Fourier analysis[19], the CGMV method[6], the stationary phase method[33], the pass counting method[30], and the generating function methods[15, 31]. These methods are epoch-making, however, there are a lot of strict conditions. For example, we can only analyze space-homogeneous QWs by the Fourier analysis[19]. Motivated by the past studies, we take advantage of two kinds of the generating function methods[15, 31]. There is a possibility to analyze various kinds of space-inhomogeneous QWs by the methods, however, it has not been clear the types of QWs that can be analyzed by the generating function methods. We can also analyze inhomogeneous QWs via the CGMV method, still the CGMV method allows only for the general discussion of localization properties for the typical QWs with one defect on the line. One of the generating function methods offers not only the time-averaged limit theorem which describes localization, but also the weak convergence theorem for QWs. The other generating function method provides the stationary measure which corresponds to the stationary distribution. It is the first application of the generating function methods for the analysis of inhomogeneous QW without defect.

Next, we study topological invariants of the complete two-phase QW. So far, coin operators whose matrix elements are real numbers are mostly employed to study the topological invariant of quantum walks, since these coin operators apparently satisfy necessary conditions required from relevant symmetries to establish a non-trivial topological invariant. However, we present that, by applying a proper unitary transform into the time-evolution operator, the coin operator with complex numbers of the complete two-phase QW can satisfy the condition. Furthermore, we find that, since this unitary transform should be applied to the whole space of the complete two-phase QW, the bulk-edge correspondence predicting the localized states, is applicable when the phases of the two-phase QW satisfy a specific condition, nevertheless the time-averaged limit measure shows the presence of localized states unless the QW is homogeneous.

Taking into account the mathematical rigorous results and the topological invariant of the complete two-phase QW, we argue the relation between the localization of the complete two-phase QW and the topological invariant with a help of the bulk-edge correspondence. We confirm that the bulk-edge correspondence agrees well with theorems for the stationary and the time-averaged limit measures. We also clarify the symmetry preserving perturbative coin operator for the complete two-phase QW. Accordingly, we clarify the relation of localization of the two-phase QW with one defect and one of the complete two-phase QW.

The rest of this paper is organized as follows. In Section 2, we define the complete two-phase QW which is the main target in this paper, and present our mathematically rigorous results. The topological invariant of the corresponding time-evolution operator is studied in Section 3. Then, we present several examples to argue our results in Section 4. Section 5 is devoted to conclusions.

2 Model and mathematically rigorous results

In this section, we first give the definition of the complete two-phase QW, and then present mathematically rigorous results on the stationary, the time-averaged limit, and the weak limit measures.

2.1 the complete two-phase QW

In this paper, we treat a two-state discrete-time QW in one dimension whose one-time step is defined by a unitary time-evolution operator $U^{(s)}$:

$$U^{(s)} = SU_x. \tag{1}$$

where S is called *the standard shift operator* defined by

$$S = \sum_x (|x\rangle\langle x+1| \otimes |L\rangle\langle L| + |x\rangle\langle x-1| \otimes |R\rangle\langle R|), \tag{2}$$

and U_x is called *the coin operator* expressed by

$$U_x = \begin{cases} \frac{1}{\sqrt{2}} \begin{bmatrix} 1 & e^{i\sigma_+} \\ e^{-i\sigma_+} & -1 \end{bmatrix} & (x \geq 0) \\ \\ \frac{1}{\sqrt{2}} \begin{bmatrix} 1 & e^{i\sigma_-} \\ e^{-i\sigma_-} & -1 \end{bmatrix} & (x \leq -1) \end{cases}, \tag{3}$$

with $\sigma_\pm \in [0, 2\pi)$. As a discrete-time QW, the walker has a coin state at position x and time t expressed by a two-dimensional vector:

$$\Psi_t(x) = \begin{bmatrix} \Psi_t^L(x) \\ \Psi_t^R(x) \end{bmatrix} \in \mathbb{C}^2 \quad (x \in \mathbb{Z} \quad \Psi_t^L(x), \Psi_t^R(x) \in \mathbb{C}),$$

where $\mathbb{C}$ is the set of complex numbers, and $\mathbb{Z}$ is the set of integers. We should note that the walker steps to the left or right according to the recurrence formula

$$\begin{aligned} \Psi_{t+1}(x) &= U_x \Psi_t(x) \\ &= P_{x+1}\Psi_t(x+1) + Q_{x-1}\Psi_t(x-1) \quad (x \in \mathbb{Z}), \end{aligned}$$

where

$$P_x = \begin{cases} \frac{1}{\sqrt{2}} \begin{bmatrix} 1 & e^{i\sigma_+} \\ 0 & 0 \end{bmatrix} & (x \geq 0) \\ \\ \frac{1}{\sqrt{2}} \begin{bmatrix} 1 & e^{i\sigma_-} \\ 0 & 0 \end{bmatrix} & (x \leq -1) \end{cases}, \quad Q_x = \begin{cases} \frac{1}{\sqrt{2}} \begin{bmatrix} 0 & 0 \\ e^{-i\sigma_+} & -1 \end{bmatrix} & (x \geq 0) \\ \\ \frac{1}{\sqrt{2}} \begin{bmatrix} 0 & 0 \\ e^{-i\sigma_-} & -1 \end{bmatrix} & (x \leq -1) \end{cases},$$

with $U_x = P_x + Q_x$.

We note that P_x and Q_x correspond to the left and right movements, respectively, and the walker steps differently in the spatial regions with the phase parameters σ_+ and σ_-, that is, $x \geq 0$ and $x \leq -1$. The QW does not have defect at the origin, which is in marked contrast to the two-phase QW with one defect[13, 14]. Hereafter, we call the QW *the complete two-phase QW*. Putting $\sigma_+ = \sigma_- = 0$, the model becomes the Hadamard walk, which has

already been intensively studied[31, 29]. At first, we derive limit theorems concerning localization for our QW, that is, the stationary and time-averaged limit measures. Then, we show the weak convergence theorem describing the ballistic spreading in the distribution of the position in a re-scaled space, which contributes to mathematically express the whole description of the behavior of the walker in the long-time limit. We also show numerical results for some concrete phase parameters and initial states to see what our analytical results suggest, especially, to relate the complete two-phase QW to the topological phases in Section 4.

2.2 rigorous result 1*: the stationary measure*

In this subsection, we present the first of our rigorous results, the stationary measure of the complete two-phase QW.

By employing P_x and Q_x, the time-evolution operator $U^{(s)}$ is written in the matrix form:

$$U^{(s)} = SU_x = \begin{bmatrix} \ddots & \vdots & \vdots & \vdots & \vdots & \cdots \\ \cdots & O & P_{-1} & O & O & O\cdots \\ \cdots & Q_{-2} & O & P_0 & O & O\cdots \\ \cdots & O & Q_{-1} & O & P_1 & O\cdots \\ \cdots & O & O & Q_0 & O & P_2\cdots \\ \cdots & O & O & O & Q_1 & O\cdots \\ \cdots & \vdots & \vdots & \vdots & \vdots & \ddots \end{bmatrix} \quad with \quad O = \begin{bmatrix} 0 & 0 \\ 0 & 0 \end{bmatrix}.$$

Now let us consider the eigenvalue problem

$$U^{(s)}\Psi = \lambda\Psi, \tag{4}$$

where λ ($\in \mathbb{C}$) with a restriction $|\lambda| = 1$ is the eigenvalue of $U^{(s)}$ and Ψ is the eigenvector defined by

$$\Psi = {}^T\left[\cdots, \begin{bmatrix}\Psi^L(-1)\\ \Psi^R(-1)\end{bmatrix}, \begin{bmatrix}\Psi^L(0)\\ \Psi^R(0)\end{bmatrix}, \begin{bmatrix}\Psi^L(1)\\ \Psi^R(1)\end{bmatrix}, \cdots\right] \in (\mathbb{C}^2)^\infty,$$

where T means the transposed operation. First of all, we give the stationary measure of our complete two-phase QW. The stationary measure at position $x \in \mathbb{Z}$ is defined by $\mu(x) = |\Psi^L(x)|^2 + |\Psi^R(x)|^2$ [15]. The derivation of Theorem 1 is based on the *splitted generating function method* (the SGF method)[15], which is provided in Appendix A.

Theorem 1 *Put*

$$\begin{cases} p = e^{i\sigma_+}(e^{-2i\sigma_-} - e^{-2i\sigma_+} - 4e^{-2i\tilde{\sigma}}) \\ q = e^{-2i\sigma_-} + e^{-2i\sigma_+} - 6e^{-2i\tilde{\sigma}} \\ r^{(\pm)} = e^{-i\sigma_+} \pm e^{-i\sigma_-} \end{cases},$$

where $\tilde{\sigma} = (\sigma_+ + \sigma_-)/2$ *and* $c \in \mathbb{R}_+$ *with* $\mathbb{R}_+ = (0, \infty)$*. Then, we obtain the stationary measure depending on the eigenvalues and eigen vectors as follows:*

1. *For* $\lambda^{(1)} = \sqrt{\dfrac{p + e^{i\sigma_+}r^{(-)}\sqrt{q}}{2(-r^{(-)} - \sqrt{q})}}$ *and* $\Psi^{(1)}(0) = {}^T[\alpha,\ \beta] = {}^T\dfrac{c}{\sqrt{2}}\left[1,\ \dfrac{1}{2}(r^{(-)} + \sqrt{q})\right]$*, and* $\lambda^{(2)} = -\lambda^{(1)}$ *and*

$\Psi^{(2)}(0) = \Psi^{(1)}(0)$, *we have*

$$\mu(x) = \begin{cases} \frac{c^2}{8}\left\{4 + |r^{(-)}|^2 + |\sqrt{q}|^2 + 2\Re(\overline{r^{(-)}}\sqrt{q})\right\} \times \left|\frac{r^{(+)} - \sqrt{q}}{\sqrt{-r^{(-)} - \sqrt{q}}\sqrt{p + e^{i\sigma_+} r^{(-)}\sqrt{q}}}\right|^{2x} & (x \geq 1) \\ \frac{c^2}{8}\left\{4 + |r^{(-)}|^2 + |\sqrt{q}|^2 + 2\Re(\overline{r^{(-)}}\sqrt{q})\right\} & (x = 0) \\ \frac{c^2}{8}\left\{(1 + 4\sin^2\sigma)|r^{(-)} + \sqrt{q}|^2 + 16\sin^2\sigma + 4\Re\{(e^{\sigma_+} - e^{i\sigma_-})\sqrt{q}\}\right\} & \\ \times\left|\frac{r^{(+)} - \sqrt{q}}{\sqrt{-r^{(-)} - \sqrt{q}}\sqrt{p + e^{i\sigma_+} r^{(-)}\sqrt{q}}}\right|^{2|x|} & (x \leq -1) \end{cases}.$$

2. *For* $\lambda^{(3)} = \sqrt{\frac{p - e^{i\sigma_+} r^{(-)}\sqrt{q}}{2(-r^{(-)} + \sqrt{q})}}$ *and* $\Psi^{(3)}(0) = {}^T[\alpha,\ \beta] = {}^T\frac{c}{\sqrt{2}}\left[1,\ \frac{1}{2}(r^{(-)} - \sqrt{q})\right]$, *and* $\lambda^{(4)} = -\lambda^{(3)}$ *and* $\Psi^{(3)}(0) = \Psi^{(4)}(0)$, *we have*

$$\mu(x) = \begin{cases} \frac{c^2}{8}\left\{4 + |r^{(-)}|^2 + |\sqrt{q}|^2 - 2\Re(\overline{r^{(-)}}\sqrt{q})\right\} \times \left|\frac{r^{(+)} + \sqrt{q}}{\sqrt{-r^{(-)} + \sqrt{q}}\sqrt{p - e^{i\sigma_+} r^{(-)}\sqrt{q}}}\right|^{2x} & (x \geq 1) \\ \frac{c^2}{8}\left\{4 + |r^{(-)}|^2 + |\sqrt{q}|^2 - 2\Re(\overline{r^{(-)}}\sqrt{q})\right\} & (x = 0) \\ \frac{c^2}{8}\left\{(1 + 4\sin^2\sigma)|r^{(-)} - \sqrt{q}|^2 + 16\sin^2\sigma - 4\Re\{(e^{\sigma_+} - e^{i\sigma_-})\sqrt{q}\}\right\} & \\ \times\left|\frac{r^{(+)} + \sqrt{q}}{\sqrt{-r^{(-)} + \sqrt{q}}\sqrt{p - e^{i\sigma_+} r^{(-)}\sqrt{q}}}\right|^{2|x|} & (x \leq -1) \end{cases}.$$

The proof of Theorem 1 is given in Appendix A. We should note that the stationary measure does not have an origin symmetry in general, however, is attenuated or diverged exponentially for the position with the same decay or divergence rate both in $x \geq 1$ and $x \leq -1$. We should note that $\sum_{x\in\mathbb{Z}} \mu(x)$ strongly depends on $c(\in \mathbb{R}_+)$, and by choosing appropriate c and $\lambda^{(j)}$ $(j = 1, 2, 3, 4)$,

$$\sum_{x\in\mathbb{Z}} \mu(x) < 1$$

holds, which indicates that there is a possibility that we can investigate localization also by the stationary measure.

2.3 rigorous result 2: the time-averaged limit measure

Let $P(X_t = x)$ be the probability that the walker exists at position x at time t, where $\{X_t\}$ is a set which is defined by $P(X_t = x) = \|\Psi_t(x)\|^2$. Then, localization of one-dimensional QWs is defined by

$$\lim_{t\to\infty} \sup P(X_t = 0) > 0.$$

Furthermore, localization can be also mathematically described by the time-averaged limit measure[16]. More explicitly, the QW starting at the origin shows localization if and only if $\overline{\mu}_\infty(0)$ is strictly positive:

$$\overline{\mu}_\infty(0) = \lim_{T\to\infty} \frac{1}{T} \sum_{t=0}^{T-1} P(X_t = 0) > 0.$$

Now we give the time-averaged limit measure for the complete two-phase QW, the second of the rigorous results in our study. Let $\varphi_0 = {}^T[\alpha, \beta]$ be the initial coin state, where $\alpha, \beta \in \mathbb{C}$, and $\overline{\mu}_\infty(x)$ be the time-averaged limit measure at position $x \in \mathbb{Z}$. Throughout this work, we assume that the walker starts at the origin, and we put $\alpha = ae^{i\phi_1},\ \beta = be^{i\phi_2}$ with $a,\ b \geq 0$, $a^2 + b^2 = 1$, and $\phi_j \in \mathbb{R}$ $(j = 1, 2)$, where $a, b \in \mathbb{R}$. Here $\mathbb{R}$ is the set of real numbers.

Theorem 2 *Put $\sigma = (\sigma_+ - \sigma_-)/2$ and $\tilde{\phi}_{12} = \phi_1 - \phi_2$. Then, we have*

$$\begin{aligned}
\overline{\mu}_\infty(x) \ =\ & \frac{2(1-\sqrt{2}a^{(+)}(\sigma))^2}{(3-2\sqrt{2}a^{(+)}(\sigma))^{|x|+2}\left\{5+\cos 2\sigma - 2\sqrt{2}b^{(+)}(\sigma) - 2\sqrt{2}a^{(+)}(\sigma)\right\}} I_{a^{(+)}(\sigma)\leq 1/\sqrt{2}}(\sigma) \\
& \times \left\{\delta_0(x)\zeta^{(+)}(\sigma) + (1-\delta_0(x))\left\{\kappa^{(+)}(\sigma)I_{x>0}(x) + \gamma^{(+)}(\sigma)I_{x<0}(x)\right\}\right\} \\
& + \frac{2(1-\sqrt{2}a^{(-)}(\sigma))^2}{(3-2\sqrt{2}a^{(-)}(\sigma))^{|x|+2}\left\{5+\cos 2\sigma - 2\sqrt{2}b^{(-)}(\sigma) - 2\sqrt{2}a^{(-)}(\sigma)\right\}} I_{a^{(-)}(\sigma)\leq 1/\sqrt{2}}(\sigma) \\
& \times \left\{\delta_0(x)\zeta^{(-)}(\sigma) + (1-\delta_0(x))\left\{\kappa^{(-)}(\sigma)I_{x>0}(x) + \gamma^{(-)}(\sigma)I_{x<0}(x)\right\}\right\},
\end{aligned} \tag{5}$$

where

$$\begin{cases}
a^{(\pm)}(\sigma) = \cos t^{(\pm)}(\sigma),\ b^{(\pm)}(\sigma) = \cos(2\sigma + t^{(\pm)}(\sigma)), \\
\zeta^{(\pm)}(\sigma) = 2 - \sqrt{2}\left\{a^2\cos(2\sigma + t^{(\pm)}(\sigma)) + b^2\cos t^{(\pm)}(\sigma)\right\} \\
\qquad\qquad -\sqrt{2}ab\left\{\cos(\tilde{\phi}_{12} - \sigma_+ - t^{(\pm)}(\sigma)) - \cos(\tilde{\phi}_{12} - \sigma_- + t^{(\pm)}(\sigma))\right\}, \\
\kappa^{(\pm)}(\sigma) = (2 - \sqrt{2}a^{(\pm)}(\sigma)) \\
\qquad\qquad \times \left\{1 + 2a^2 - 2\sqrt{2}a^2\cos(2\sigma + t^{(\pm)}(\sigma)) - 2ab\cos(\tilde{\phi}_{12} - \sigma_+) + 2\sqrt{2}ab\cos(\tilde{\phi}_{12} - \sigma_- + t^{(\pm)}(\sigma))\right\}, \\
\gamma^{(\pm)}(\sigma) = (2 - \sqrt{2}a^{(\pm)}(\sigma)) \\
\qquad\qquad \times \left\{1 + 2b^2 - 2\sqrt{2}b^2\cos t^{(\pm)}(\sigma) + 2ab\cos(\tilde{\phi}_{12} - \sigma_+) - 2\sqrt{2}ab\cos(\tilde{\phi}_{12} - \sigma_+ - t^{(\pm)}(\sigma))\right\}.
\end{cases}$$

with

$$t^{(\pm)}(\sigma) = \varphi^{(\pm)}(\sigma) - \sigma.$$

Here $\varphi^{(\pm)}(\sigma)$ is defined by

$$\begin{cases} \cos\varphi^{(\pm)}(\sigma) = \dfrac{1}{\sqrt{2}}\cos\sigma, \\ \\ \sin\varphi^{(\pm)}(\sigma) = \pm\sqrt{1-\dfrac{1}{2}\cos^2\sigma}. \end{cases}$$

We emphasize that the time-averaged limit measure has an exponential decay for the position. Moreover, the time-averaged limit measure does not have an origin symmetry, which is in marked contrast to that of the two-phase QW with one defect[13]. In other words, the result indicates that the defect at the origin may contribute to the symmetric time-averaged distribution. Here to clarify the relation between the stationary and time-averaged limit measures has been one of the mathematically basic interesting problems. In addition, our result suggests that if $\sigma_+ \neq \sigma_-$, then, the decay rate is positive valued, i.e., $1/(3-2\sqrt{2}a^{(\pm)}(\sigma)) > 0$, which indicates that localization may happen regardless of the phase parameters σ_+ and σ_-, and initial state. We also notice that the time-averaged limit measure heavily depends on the relative phase difference $\sigma = (\sigma_+ - \sigma_-)/2$, however, is independent of each phase parameter σ_+ or σ_- if $ab = 0$.

We should remark that we can not see the probability distribution only from the time-averaged limit measure, since $\sum_{x\in\mathbb{Z}} \overline{\mu}_\infty(x) < 1$ holds. Appendix B is devoted to the derivation of Theorem 2.

2.4 rigorous result 3: the weak convergence theorem

Put

$$C = \sum_x \overline{\mu}_\infty(x),$$

where $\overline{\mu}_\infty(x)$ is the time-averaged limit measure at position $x \in \mathbb{Z}$ obtained by Theorem 2. From now on, we present the weak convergence theorem for the missing part $1-C$ with $0 \leq C \leq 1$. In general, the weak convergence theorem describes the ballistic behavior of the QW[29]. Throughout this subsection, we assume that the walker starts from the origin with the initial coin state $\varphi_0 = {}^T[\alpha, \beta]$, where $\alpha, \beta \in \mathbb{C}$. Put $\alpha = ae^{\phi_1},\ \beta = be^{\phi_2}$ with $a, b \geq 0,\ a^2+b^2 = 1$ and $\phi_1, \phi_2 \in \mathbb{R}$.

Theorem 3 *Let $\tilde{\phi}_{12} = \phi_1 - \phi_2$. For the complete two-phase QW, X_t/t converges weakly to the random variable Z which has the following density function:*

$$\mu(x) = C\delta_0(x) + w(x) f_K(x; 1/\sqrt{2}), \tag{6}$$

where

$$f_K(x; 1/\sqrt{2}) = \frac{1}{\pi(1-x^2)\sqrt{1-2x^2}},$$

and

$$w(x) = \begin{cases} \dfrac{t_2^{(+)}x^3 + t_1^{(+)}x^2}{s_1x^2 + s_0} & (x \geq 0), \\ \\ \dfrac{t_2^{(-)}x^3 + t_1^{(-)}x^2}{s_1x^2 + s_0} & (x < 0), \end{cases} \tag{7}$$

with

$$\begin{cases} s_1 = \cos^2\sigma, \quad s_0 = \sin^2\sigma, \\ t_2^{(+)} = 1 - 2a^2 - 2ab\cos(\tilde{\phi}_{12} - \sigma_+),\ t_2^{(-)} = 1 - 2a^2 - 2ab\cos(\tilde{\phi}_{12} - \sigma_+), \\ t_1^{(+)} = 1 + 4a^2\sin^2\sigma - 2ab\left\{\cos(\tilde{\phi}_{12} - \sigma_+) - \cos(\tilde{\phi}_{12} - \sigma_-)\right\}, \\ t_1^{(-)} = 1. \end{cases}$$

Here $w(x)f_K(x; 1/\sqrt{2})$ is an absolutely continuous part of $\mu(x)$. We emphasize that the weak limit measure is generally asymmetric for the origin, and heavily depends on the phase parameters and initial state. Furthermore, like the time-averaged limit measure, if $ab = 0$, then, the weak limit measure becomes independent of each phase parameter σ_+ or σ_-, in other words, we can write down the weight function $w(x)$ by the relative phase difference σ and initial state. We provide with the proof of Theorem 3 in Appendix C by using the *time-space generating function method*[31].

3 Topological invariants of the complete two-phase QW

In this section, we investigate the topological invariant of the complete two-phase QW.

As we derived in the previous section, the time-averaged limit measure of the complete two-phase QW exhibits localization around the origin. Recently, there has been a development to understand localization of QWs as a localized surface state originating to the topological invariant which is inherited from the time-evolution operator[28, 25, 27]. In order to relate the topological invariant to the localized states, we use a fundamental principle, called the *bulk-edge correspondence*. This principle states that an absolute value of difference of topological numbers in two adjacent spatial regions gives a lower limit of the number of eigenvalues/eigenvectors exhibiting localization in the vicinity of the interface. It would be very interesting to directly compare the mathematically derived stationary and time-averaged limit measures with the prediction of the bulk-edge correspondence, which motivates us to derive the topological invariants of the complete two-phase QW.

3.1 relevant symmetries of the time-evolution operator to establish topological phases

Since each spatial region of the complete two-phase QW should be characterized by own topological number, we separately calculate the topological number on the regions with the phase σ_+ or σ_- in the coin operator. First, we calculate the topological number for the region with the phase σ_+. Put the coin operator for $x \geq 0$ as

$$U_+ = \frac{1}{\sqrt{2}}\begin{bmatrix} 1 & e^{i\sigma_+} \\ e^{-i\sigma_+} & -1 \end{bmatrix}.$$

We assume that the whole of line has the same coin U_+, because the calculation of the topological number is simplified for a system with translation symmetry. Topological invariant for the region $x \leq -1$ is easily obtained from the result for $x \geq 0$ by replacing σ_+ with σ_-.

In the argument of the ordinary topological phase of matter, it is important to identify symmetries of the system, that is, time-reversal, particle-hole, and chiral symmetries[5, 10, 20, 37]. We call these three symmetries *relevant symmetries for topological phases*. While these symmetries give constraints on the Hamiltonian, now we derive the corresponding constraints on the time-evolution operator of QWs. The detail of the derivation is explained in Appendix D. In order to make clear the relation to physics, we introduce quasi-energy $\varepsilon \in \mathbb{R}$, by the terminology

in physics, which is defined from the eigenvalue λ of the time-evolution operator in Eq. (4) as

$$\lambda = e^{-i\varepsilon},$$

Note that quasi-energy ε has 2π periodicity. The conditions required from the relevant symmetries for topological phases on the time-evolution operator are summarized as

$$T\,U^{(s)}\,T^{-1} = \left(U^{(s)}\right)^{-1} \quad \text{(Time-reversal symmetry)}, \tag{8}$$

$$P\,e^{i\varepsilon_P}U^{(s)}\,P^{-1} = e^{i\varepsilon_P}\cdot U^{(s)} \quad \text{(Particle-hole symmetry)}, \tag{9}$$

$$\Gamma\,e^{i\varepsilon_\Gamma}U^{(s)}\,\Gamma^{-1} = \left(e^{i\varepsilon_\Gamma}\cdot U^{(s)}\right)^{-1} \quad \text{(Chiral symmetry)}\ . \tag{10}$$

Here the symmetry operators T and P are anti-unitary operators (i.e., they should contain a complex conjugate operator K), while Γ is a unitary one. In Eqs. (9) and (10), we assume that the time-evolution operator $U^{(s)}$ satisfies the eigenvalue equation $e^{i\varepsilon_X}U^{(s)}\Psi = e^{i\varepsilon}\Psi$, where X stands for P or Γ, with an eigenvector Ψ and $\varepsilon_P, \varepsilon_\Gamma \in \mathbb{R}$. If so, Eqs. (9) and (10) guarantee that $e^{i\varepsilon_X}U^{(s)}(X\Psi) = e^{-i\varepsilon}(X\Psi)$. Therefore, a pair of quasi-energies with opposite signs $\pm\varepsilon$ around the symmetric point ε_P and/or ε_Γ appears. Generally, ε_P and ε_Γ are set to be zero, however, let us consider arbitrary values, because the recent work on the topological phase of Hadamard walks [35] pointed out its importance.

As explained in Ref. [4], in order to clarify symmetries of the time-evolution operator, we should redefine the time-evolution operator by shifting the origin of time to fit in the *symmetry time frame*. For our QW, this corresponds to the situation that a half of the first coin operation is absorbed into the initial state. Then, the redefined time-evolution operator for the one-time step is expressed as

$$U_+^{(s)} = (U_+)^{1/2}\,S\,(U_+)^{1/2}.$$

As explained in Appendix E, by employing $U_+^{(s)}$ and setting proper symmetric point of quasi-energies, we identify the symmetry operators satisfying particle-hole and chiral symmetries in Eqs. (9) and (10), respectively:

$$P = \sum_x |x\rangle\langle x| \otimes \left(V_{\sigma'}\cdot\tau_0\,K\cdot V_{\sigma'}^{-1}\right) \quad \text{with } \varepsilon_P = 0, \tag{11}$$

$$\Gamma = \sum_x |x\rangle\langle x| \otimes \left(V_{\sigma'}\cdot\tau_1\cdot V_{\sigma'}^{-1}\right) \quad \text{with } \varepsilon_\Gamma = -\pi/2, \tag{12}$$

where

$$V_{\sigma'} = \begin{bmatrix} e^{i\sigma'/2} & 0 \\ 0 & e^{-i\sigma'/2} \end{bmatrix}, \quad \sigma' = \sigma_+ \tag{13}$$

A two-dimensional identity matrix τ_0 and Pauli matrices

$$\tau_1 = \begin{bmatrix} 0 & 1 \\ 1 & 0 \end{bmatrix}, \quad \tau_2 = \begin{bmatrix} 0 & -i \\ i & 0 \end{bmatrix}, \quad \tau_3 = \begin{bmatrix} 1 & 0 \\ 0 & -1 \end{bmatrix},$$

act on the coin space. We note that, while $\sigma' = \sigma_+ + m\pi$ ($m \in \mathbb{Z}$) is a more general expression of σ' in Eq. (13), we fix $m = 0$ for simplicity.

While both chiral and particle-hole symmetries of the time-evolution operator can be identified, the values of ε_P and ε_Γ in Eqs. (11) and (12) are different. This means that the time-evolution operator does not possess both chiral and particle-hole symmetries at the same symmetric point of quasi-energy. If two of the three relevant

symmetries for topological phases are established, the other symmetry is automatically confirmed by combining the two identified symmetry operators. In our case, either chiral or particle-hole symmetries is established at a specific quasi-energy. Thereby, time-reversal symmetry cannot be retained.

For further arguments, we need to choose the symmetric point of quasi-energy, that is, $\varepsilon_P = 0$ or $\varepsilon_\Gamma = -\pi/2$.

The proper symmetric point of quasi-energy to study topological invariant can be chosen from the distribution of the eigenvalue of $U_+^{(s)}$, because the topological numbers can be well defined unless absolutely continuous spectra exist at the symmetric points of quasi-energy, i.e., the quasi-energy gap should open by the terminology in physics. In Appendix F, the eigenvalue problem of homogeneous $U_+^{(s)}$ is solved by the Fourier analysis. We obtain the eigenvalue

$$\begin{aligned} \lambda = e^{i[\pm\varepsilon(k)+\pi/2]} &= i[\cos\{\varepsilon(k)\} \pm i\sin\{\varepsilon(k)\}], \\ \cos[\varepsilon(k)] &= \sin(k)/\sqrt{2}, \end{aligned} \tag{14}$$

where $k \in [0 : 2\pi)$ is the wave number. We see that the absolutely continuous spectra include quasi-energy $\varepsilon = 0, \pi$ ($\lambda = \pm 1$), however, do not exist at $\varepsilon = \pm\pi/2$ ($\lambda = \pm i$). Therefore, we focus on the time-evolution operator possessing chiral symmetry, where the topological numbers are well defined due to the presence of the quasi-energy gap. Therefore, the time-evolution operator $U_+^{(s)}$, we focus on hereafter in this section, possesses only chiral symmetry, and then belongs to the chiral unitary class (class AIII in the Cartan classification). In the table of the classification of topological phases[39], it is known that class AIII can possess $\mathbb{Z}$ topological phases in the one dimensional system.

3.2 topological invariants and the bulk-edge correspondence

Having identified that the system possesses chiral symmetry, topological invariants for the above time-evolution operator are given by calculating winding numbers[4]. Because of 2π periodicity of quasi-energy, we remark that the QW with chiral or particle-hole symmetries possesses two symmetric points of the quasi-energy at $\varepsilon_\Gamma = -\pi/2$ as well as at $\varepsilon_\Gamma + \pi = \pi/2$. Thus, we need to introduce two topological numbers. For the spatial region $x \geq 0$, topological numbers $\nu^+_{\pm\pi/2}$ at quasi-energies $\varepsilon = \pm\pi/2$ ($\lambda = \mp i$) are derived as

$$(\nu^+_{-\pi/2}, \nu^+_{+\pi/2}) = (1, 0). \tag{15}$$

The detail of the calculation is presented in Appendix F.

Topological invariants for the spatial region $x \leq -1$ of the complete two-phase QW are obtained by applying Eq. (15) with a replacement σ_+ with σ_-. However, we should keep using the same chiral symmetry operator Γ for the whole of the system, otherwise chiral symmetry is broken. In other words, the same σ' in $V_{\sigma'}$ has to be applied for $x \geq 0$ and $x \leq -1$. This restricts the phase σ_- so as to satisfy

$$\sigma_- = \sigma_+ + n\pi \quad (n \in \mathbb{Z}), \tag{16}$$

to maintain chiral symmetry. According to Appendix F, topological numbers $\nu^-_{\pm\pi/2}$ at quasi-energies $\varepsilon = \pm\pi/2$ for the spatial region with $x \leq -1$ are summarized as

$$(\nu^-_{-\pi/2}, \nu^-_{+\pi/2}) = \begin{cases} (1,0) & n: \text{ even}, \\ (0,1) & n: \text{ odd}. \end{cases} \tag{17}$$

As we mentioned at the beginning of this section, the bulk-edge correspondence predicts a minimum number of localized states from the absolute value of the difference of topological numbers of adjacent two regions. Thereby, on one hand, when n is even, the two regions have the same topological numbers $(\nu^\pm_{-\pi/2}, \nu^\pm_{+\pi/2}) = (1, 0)$, and then

localized eigenstates are not expected from the bulk-edge correspondence. On the other hand, when n is odd, the two regions have different topological numbers whose difference is $|\nu^{+}_{\pm\pi/2} - \nu^{-}_{\pm\pi/2}| = 1$, and then, two localized eigenstates, one at $\varepsilon = -\pi/2$ ($\lambda = i$) and the other at $\varepsilon = \pi/2$ ($\lambda = -i$), in the vicinity of the origin are predicted by the bulk-edge correspondence.

If n in Eq. (16) is not an integer, chiral symmetry of the two-phase QW is broken. In this case, localized states at $\varepsilon = \pm\pi/2$ originating to the topological invariant are not expected from the bulk-edge correspondence. While this does not exclude a possibility having localized states at $\varepsilon = \pm\pi/2$ since the bulk-edge correspondence gives a lower bound of the number of edge states. However, most generally, quasi-energy of such localized states deviates from $\varepsilon = \pm\pi/2$.

3.3 robustness of localized states by topological protections

One of the important properties of localized states originating to the topological invariant is robustness against perturbations satisfying the following conditions;

1. the perturbation should preserve the same relevant symmetries for topological phases with the non-perturbative time-evolution operator.

2. the perturbation remains quasi-energy gaps open.

In case of one dimension, this robustness can be expressed more clearly such that the eigenvalue of the localized state remains unchanged and the eigenvector remains localized under the perturbations. Therefore, this property can be utilized to verify whether localized states at $\varepsilon = \pm\pi/2$ originate to the topological invariant or not.

Now we consider the perturbations for the complete two-phase QW. We assume that only the coin operator introduces the perturbation. Since the complete two-phase QW possesses chiral symmetry, we need to show that the perturbative coin operator should also satisfy the condition demanded from chiral symmetry. Taking account of Eqs. (10) and (12), the coin operator U_p, as a source of perturbation, should satisfy the following relation:

$$\Gamma U_p \tau_3 \Gamma^{-1} = (U_p \tau_3)^{-1} \tag{18}$$

We identify that the coin operator U_p with the position dependent parameters $\theta_x, \omega_x \in [0, 2\pi)$ satisfies Eq. (18):

$$U_p(\theta_x, \omega_x) = \begin{bmatrix} e^{i\omega_x}\cos(\theta_x) & e^{i\sigma_p}\sin(\theta_x) \\ e^{-i\sigma_p}\sin(\theta_x) & -e^{-i\omega_x}\cos(\theta_x) \end{bmatrix}, \quad \sigma_p = \sigma_+ \text{ or } \sigma_-. \tag{19}$$

We note that, when $\theta_x = \pi/4$, $\omega_x = 0$, and $\sigma_p = \sigma_+$ or σ_-, U_p is identical with the coin operator of the complete two-phase QW. We examine robustness of localized states by employing the perturbative coin operator U_p with random θ_x in the next section.

4 Relation between localization and topological invariants

In this section, we show several examples of the complete two-phase QW with specific phases to see what our analytical results suggest. Especially, we argue the relation between localization and topological invariants of the complete two-phase QW. In addition, we investigate the relation to the two-phase QW with one defect.

4.1 in case of the homogeneous QW

At first, we consider the space-homogeneous QW whose quantum coin is given by

$$U = \frac{1}{\sqrt{2}} \begin{bmatrix} 1 & i \\ -i & -1 \end{bmatrix}, \tag{20}$$

which is obtained by putting $\sigma_+ = \sigma_- = \pi/2$ in Eq. (3). Let the initial coin state be $\varphi_0 = {}^T[\alpha, \beta]$ at the origin, where $\alpha, \beta \in \mathbb{C}$ with $|\alpha|^2 + |\beta|^2 = 1$. By Theorem 2, we get the time-averaged limit measure by

$$\overline{\mu}_\infty(x) = 0 \quad (x \in \mathbb{Z}),$$

and as a result, we obtain the coefficient of the delta function in Eq. (6) by

$$C = \sum_x \overline{\mu}_\infty(x) = 0. \tag{21}$$

Therefore, we see that localization does not happen for the homogeneous QW, which agrees with the previous study [31].

We also obtain the weight function in Eq. (6) from Theorem 3 by

$$w(x) = (1 - 2a^2 - 2ab \sin \tilde{\phi}_{12})x + 1.$$

Now we focus on the stationary measure. According to Theorem 1, we have in this case the eigenvalues $\lambda^{(1)} = \sqrt{-i}$, $\lambda^{(2)} = -\lambda^{(1)}$, $\lambda^{(3)} = \sqrt{i}$, and $\lambda^{(4)} = -\lambda^{(3)}$, and we also obtain the stationary measure by

$$\mu(x) = c^2 \tag{22}$$

for all $x \in \mathbb{Z}$. Taking account of $\overline{\mu}_\infty(x) = 0$, we see that both the time-averaged and stationary measures do not have exponential decay, which may imply that the uniformity of the stationary measure suggests non-localization.

In Fig. 1, we show the numerical results of probability distribution at time 10000 in re-scaled space $(x/10000, 10000P_{10000}(x))$ for the cases of ${}^T[\alpha, \beta] = {}^T[1, 0]$, where x expresses the position of the walker and $P_{10000}(x)$ represents the probability that the walker exists on position x at time 10000. We should note that $x/10000$ and $10000P_{10000}(x)$ correspond to the horizontal and vertical axes, respectively. At the same time, we plot $w(x)f_K(x; 1/\sqrt{2})$ representing an absolutely continuous part of the weak-limit measure, in Fig. 1. We see that the curve representing $w(x)f_K(x; 1/\sqrt{2})$ seems to be on the middle of the probability distribution on each position, which indicates that our analytical result is mathematically proper.

We also numerically solve the eigenvalue problem of the complete two-phase QW with the coin operator in Eq. (20) *on the path*[22], i.e., in the finite position space in the range of $-N \leq x \leq N-1$ with $N = 100$. The QW on the path has the finite number of bases

$$\{|-N, R\rangle, |-N+1, L\rangle, |-N+1, R\rangle, \cdots, |N-2, L\rangle, |N-2, R\rangle, |N-1, L\rangle\},$$

and the coin and shift operators are modified as follows:

$$\begin{aligned} U &= \sum_{x=-N+1}^{N-2} |x\rangle\langle x| \otimes U_x \\ &\quad + \frac{1}{\sqrt{2}} e^{-i\sigma_-} |-N\rangle\langle -N| \otimes |R\rangle\langle R| + \frac{1}{\sqrt{2}} e^{i\sigma_+} |N-1\rangle\langle N-1| \otimes |L\rangle\langle L|, \\ S &= \sum_{x=-N+1}^{N-2} \Big(|x\rangle\langle x+1| \otimes |L\rangle\langle L| + |x\rangle\langle x-1| \otimes |R\rangle\langle R| \Big) \\ &\quad + |-N\rangle\langle -N+1| \otimes |R\rangle\langle L| + |N-1\rangle\langle N-2| \otimes |L\rangle\langle R|. \end{aligned}$$

As shown in Fig. 2, all eigenvalues calculated by the numerical diagonalization of the QW on the path (green dots) are densely distributed in two regions on the unit circle and there is no apparently isolated eigenvalue. Since the calculated eigenvalues are consistent with Eq. (14) derived by the Fourier analysis, they would develop into continuous spectra in the infinite space limit.

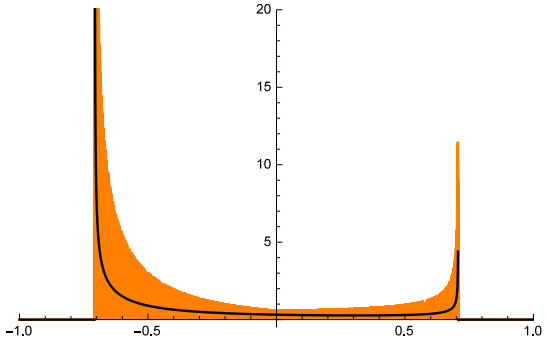

Fig. 1. ($\sigma_+ = \sigma_- = \pi/2$, ${}^T[\alpha, \beta] = {}^T[1, 0]$)
Orange curve: Probability distribution in a re-scaled space $(x/10000, 10000 P_{10000}(x))$ at time 10000. (Because the probability distribution at time 10000 is zero for odd x but finite for even x, and the position space x is heavily shrunk in the horizontal axis, the orange curve representing the probability distribution $P_{10000}(x)$ looks to fill the region.)
Black curve: $w(x) f_K(x; 1/\sqrt{2})$.

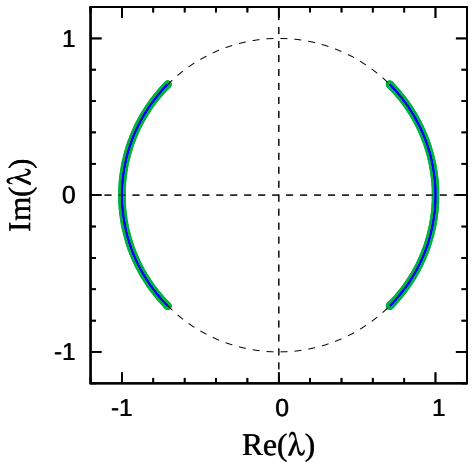

Fig. 2. ($\sigma_+ = \sigma_- = \pi/2$)
Green dense dots : Numerically calculated eigenvalues of the time-evolution operator of the homogeneous QW on the path.
Blue curves : The eigenvalues in Eq. (14).
The dashed curve represents a unit circle on the complex plane.

4.2 in case of the complete two-phase QW with chiral symmetry

Next we treat the complete two-phase QW whose quantum coin is given by

$$U_x = \begin{cases} U_+ = \dfrac{1}{\sqrt{2}} \begin{bmatrix} 1 & -i \\ i & -1 \end{bmatrix} & (x = 0, 1, 2, \cdots) \\ \\ U_- = \dfrac{1}{\sqrt{2}} \begin{bmatrix} 1 & i \\ -i & -1 \end{bmatrix} & (x = -1, -2, \cdots) \end{cases}, \tag{23}$$

We obtain the QW by putting $\sigma_+ = 3\pi/2$ and $\sigma_- = \pi/2$ in Eq. (3). Because of $\sigma_+ - \sigma_- = \pi$, the two-phase QW retains chiral symmetry associated with the symmetric point $\varepsilon_\Gamma = -\pi/2$. Taking account of Eqs. (15) and (17) and applying the bulk-edge correspondence, non-degenerate localized eigen states with eigenvalues $\lambda = \pm i$ are predicted.

Here we consider the stationary measure. Inputting $\sigma_+ = 3\pi/2$ and $\sigma_- = \pi/2$ into Theorem 1, we need to take into account the two cases, that is, $\sqrt{e^{-2i\sigma_+}} = e^{-i\sigma_+}$ and $\sqrt{e^{-2i\sigma_+}} = -e^{-i\sigma_+}$ as follows;

1. Case of $\sqrt{e^{-2i\sigma_+}} = e^{-i\sigma_+}$:
   We obtain eigenvalues $\lambda^{(1)} = \lambda^{(3)} = i$ and $\lambda^{(2)} = \lambda^{(4)} = -i$. Also, from Theorem 1, we obtain the stationary

measure for $\lambda^{(1)}$ and $\lambda^{(2)}$ by

$$\mu(x) = \begin{cases} c^2(2+\sqrt{2})\left(\dfrac{1}{3+2\sqrt{2}}\right)^x & (x \geq 1) \\ c^2(2+\sqrt{2}) & (x = 0) \\ c^2(10+7\sqrt{2})\left(\dfrac{1}{3+2\sqrt{2}}\right)^{|x|} & (x \leq -1) \end{cases}, \tag{24}$$

and that for $\lambda^{(3)}$ and $\lambda^{(4)}$ by

$$\mu(x) = \begin{cases} c^2(2-\sqrt{2})\left(\dfrac{1}{3-2\sqrt{2}}\right)^x & (x \geq 1) \\ c^2(2-\sqrt{2}) & (x = 0) \\ c^2(10-7\sqrt{2})\left(\dfrac{1}{3-2\sqrt{2}}\right)^{|x|} & (x \leq -1) \end{cases}. \tag{25}$$

2. Case of $\sqrt{e^{-2i\sigma_+}} = -e^{-i\sigma_+}$:
   We obtain eigenvalues $\lambda^{(1)} = \lambda^{(3)} = i$ and $\lambda^{(2)} = \lambda^{(4)} = -i$.
   Also, by Theorem 1, we get the stationary measure for $\lambda^{(1)}$ and $\lambda^{(2)}$ by

$$\mu(x) = \begin{cases} c^2(2-\sqrt{2})\left(\dfrac{1}{3-2\sqrt{2}}\right)^x & (x \geq 1) \\ c^2(2-\sqrt{2}) & (x = 0) \\ c^2(10-7\sqrt{2})\left(\dfrac{1}{3-2\sqrt{2}}\right)^{|x|} & (x \leq -1) \end{cases}, \tag{26}$$

   and for $\lambda^{(3)}$ and $\lambda^{(4)}$, we have

$$\mu(x) = \begin{cases} c^2(2+\sqrt{2})\left(\dfrac{1}{3+2\sqrt{2}}\right)^x & (x \geq 1) \\ c^2(2+\sqrt{2}) & (x = 0) \\ c^2(10+7\sqrt{2})\left(\dfrac{1}{3+2\sqrt{2}}\right)^{|x|} & (x \leq -1) \end{cases}. \tag{27}$$

Thereby, the eigenvalues by Theorem 1 is consistent with the prediction by the bulk-edge correspondence, while they are doubly degenerated. However, the decay rate of the stationary measure corresponding to the degenerated eigenvalues are different. From Eqs. (24)- (27), we find that, the stationary measure for one of the degenerated pair $\lambda = \pm i$ shows the exponential decay with the rate $1/(3+2\sqrt{2})$ from the origin where the topological number varies, while the other one grows exponentially with the rate $1/(3-2\sqrt{2})$ which is larger than one. The latter one

cannot be regarded as a localized state in a view point of the bulk-edge correspondence since the measure near the origin is rather small. Furthermore, from a physical viewpoint, a stationary measure exhibiting divergences of the measure for the point at infinity is generally considered as an unphysical solution because of the contradiction to the normalization condition. Hence, we can discard one of the degenerated states, which exhibits the divergent solution. Accordingly, we obtain the non-degenerated two eigenstates for $\lambda = \pm i$ and confirm the complete agreement with the prediction of bulk-edge correspondence. In addition, by rewriting Eqs. (24) and (27) as

$$\mu(x) = \begin{cases} c^2(2+\sqrt{2})\left(\dfrac{1}{3+2\sqrt{2}}\right)^x & (x \geq 0) \\ \\ c^2(2+\sqrt{2})\left(\dfrac{1}{3+2\sqrt{2}}\right)^{|x|-1} & (x \leq -1) \end{cases},$$

we clearly see that the stationary distribution with chiral symmetry is symmetric at $x = -1/2$, which is consistent with that of our numerical result (Fig. 6).

Next, we focus on the time-averaged limit measure. Let the initial coin state be $\varphi_0 = {}^T[1, 0]$. According to Theorem 2, we obtain the time-averaged limit measure by

$$\begin{aligned} \overline{\mu}_\infty(x) &= \begin{cases} \dfrac{2+\sqrt{2}}{2(3+2\sqrt{2})^{x+2}} & (x \geq 1) \\ \\ \dfrac{2+\sqrt{2}}{2(3+2\sqrt{2})^2} & (x = 0) \\ \\ \dfrac{10+7\sqrt{2}}{2(3+2\sqrt{2})^{|x|+2}} & (x \leq -1) \end{cases} \\ &= \begin{cases} \dfrac{2+\sqrt{2}}{2(3+2\sqrt{2})^{x+2}} & (x \geq 0) \\ \\ \dfrac{2+\sqrt{2}}{2(3+2\sqrt{2})^{|x|+1}} & (x \leq -1) \end{cases}, \end{aligned} \tag{28}$$

and as a result, the coefficient of the delta function is given by

$$C = \sum_x \overline{\mu}_\infty(x) = \sum_{j=1}^{\infty} \frac{2+\sqrt{2}}{2(3+2\sqrt{2})^{j+2}} + \frac{2+\sqrt{2}}{2(3+2\sqrt{2})^2} + \sum_{k=1}^{\infty} \frac{10+7\sqrt{2}}{2(3+2\sqrt{2})^{k+2}} = 0.12132... > 0. \tag{29}$$

We remark that the time-averaged limit measure in Eq. (28) is identical with the stationary measure in Eq. (24) by inputting $c^2 = 1/[2(3+2\sqrt{2})^2]$. Even from this point of view, the stationary measure exhibiting the divergence at infinity is excluded.

Owing to Theorem 3, we have the weight function of the probability distribution by

$$w(x) = \begin{cases} x^2(5-x) & (x \geq 0), \\ \\ x^2(1-x) & (x < 0). \end{cases}$$

Hence we see

$$\int_{-\frac{1}{\sqrt{2}}}^{\frac{1}{\sqrt{2}}} w(x) f_K(x; 1/\sqrt{2}) dx = 0.87868..., \tag{30}$$

which leads to

$$C + \int_{-\frac{1}{\sqrt{2}}}^{\frac{1}{\sqrt{2}}} w(x) f_K(x; 1/\sqrt{2}) dx = 1.$$

Here we present the numerical results of the time-averaged limit measure, and we see that the numerical results gradually near to our analytical result at a very low speed (Fig. 3). Next we show the numerical results of the probability distribution at time 10000 in re-scaled space $(x/10000, 10000 P_{10000}(x))$, as well as $w(x) f_K(x; 1/\sqrt{2})$, which is an absolutely continuous part of the weak limit measure $\mu(dx)$, in Fig. 4. We see that the curve representing $w(x) f_K(x; 1/\sqrt{2})$ seems to be on the middle of the probability distribution on each position, which suggests that our analytical result is mathematically correct. We should note that the weak limit measure represents the asymmetry of the probability distribution (Fig. 4). We emphasize that the walker is trapped near the origin in a short time, and the distribution form does not change after many steps.

Again, we numerically calculate the eigenvalues of the two-phase QW with the coin operator in Eq. (23) on the path in the range of $-N \leq x \leq N-1$ with $N = 100$. As shown in Fig. 5, we confirm that most eigenvalues are densely distributed on the continuous spectrum in Eq. (14). Most importantly, there exist non-degenerated two eigenvalues at $\lambda = \pm i$. We also confirm that the numerically calculated stationary measure with the eigenvalue $\lambda = i$ almost overlaps with the stationary measure in Eq. (24), as shown in Fig. 6. As we mentioned, the localized state originating to the topological invariant should be robust against perturbations of the system. We check this by using the perturbative coin operator U_p in Eq. (19). We consider that θ_x of U_p consists of two parts:

$$\theta_x = \theta_0 + \delta\theta_x,$$

which are the constant $\theta_0 = \pi/4$ and independent and identically distributed random variable $\delta\theta_x$ in the range of $[-\pi/4 : \pi/4]$. Note that we choose the rather narrow range for $\delta\theta_x$ so that the quasi-energy gaps remain open. We choose $\sigma_p = \sigma_- = \pi/2$ for $x \leq -1$ and $\sigma_p = \sigma_+ = 3\pi/2$ for $x \geq 0$, and $\omega_x = 0$ for all x. Figure 7 shows eigenvalues of the two-phase QW with the above perturbative coin on the path. We clearly see that two eigenvalues corresponding to localization at $\lambda = \pm i$ remain unchanged under the perturbation, while the others do not. Taking into account these results, we confirm the validity of the bulk-edge correspond for the complete two-phase QW with chiral symmetry.

4.3 in case of the complete two-phase QW without the relevant symmetries for topological phases

Here we focus on the complete two-phase QW whose quantum coin is expressed by

$$U_x = \begin{cases} U_+ = \dfrac{1}{\sqrt{2}} \begin{bmatrix} 1 & -1 \\ -1 & -1 \end{bmatrix} & (x = 0, 1, 2, \cdots) \\ \\ U_- = \dfrac{1}{\sqrt{2}} \begin{bmatrix} 1 & i \\ -i & -1 \end{bmatrix} & (x = -1, -2, \cdots) \end{cases}. \tag{31}$$

We obtain the QW by putting $\sigma_+ = \pi$ and $\sigma_- = \pi/2$ in Eq. (3). Because of $\sigma_+ - \sigma_- = \pi/2 \neq n\pi$ $(n \in \mathbb{Z})$, the two-phase QW does not retain any relevant symmetries for topological phases, and localized states with eigenvalues

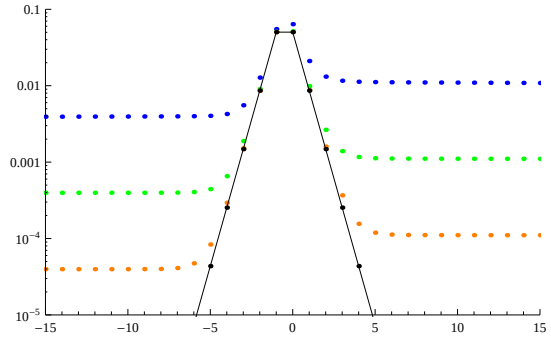

Fig. 3. ($\sigma_+ = 3\pi/2, \sigma_- = \pi/2,\ {}^T[\alpha,\beta] = {}^T[1,0]$)
Black line: the time-averaged limit measure,
Blue dotted line: time-averaged probability till time 100,
Green dotted line:time-averaged probability till time 1000,
Orange dotted line: time-averaged probability till time 10000. .

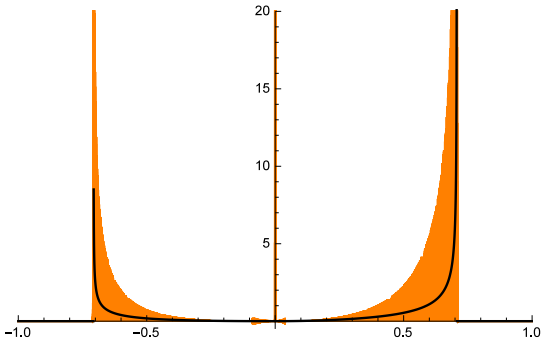

Fig. 4. ($\sigma_+ = 3\pi/2, \sigma_- = \pi/2,\ {}^T[\alpha,\beta] = {}^T[1,0]$)
Orange curve: Probability distribution in a re-scaled space $(x/10000, 10000P_{10000}(x))$ at time 10000,
Black curve: $w(x)f_K(x;1/\sqrt{2})$.

$\lambda = \pm i$ are not expected from the bulk-edge correspondence.

At first, we consider the stationary measure. By inputting $\sigma_+ = \pi$ and $\sigma_- = \pi/2$ into Theorem 1, we need to consider the next two cases;

1. Case of $\sqrt{q} = \sqrt{-6i} = \sqrt{3}(1-i)$:
   We obtain the eigenvalues
   $$\lambda^{(1)} = \sqrt{-\frac{1}{2} - \frac{\sqrt{3}}{2}i}, \qquad \lambda^{(2)} = -\lambda^{(1)},$$
   and
   $$\lambda^{(3)} = \sqrt{-\frac{1}{2} + \frac{\sqrt{3}}{2}i}, \qquad \lambda^{(4)} = -\lambda^{(3)}. \tag{32}$$
   We also obtain the stationary measure for $\lambda^{(1)}$ and $\lambda^{(2)}$ by
   $$\mu(x) = \begin{cases} \frac{c^2}{2}(3-\sqrt{3})\left(\frac{1}{2-\sqrt{3}}\right)^x & (x \geq 1) \\ \frac{c^2}{2}(3-\sqrt{3}) & (x = 0) \\ \frac{c^2}{2}(9-5\sqrt{3})\left(\frac{1}{2-\sqrt{3}}\right)^{|x|} & (x \leq -1) \end{cases}$$
   $$= \begin{cases} \frac{c^2}{2}(3-\sqrt{3})\left(\frac{1}{2-\sqrt{3}}\right)^x & (x \geq 0) \\ \frac{c^2}{2}(3-\sqrt{3})\left(\frac{1}{2-\sqrt{3}}\right)^{|x|-1} & (x \leq -1) \end{cases}, \tag{33}$$

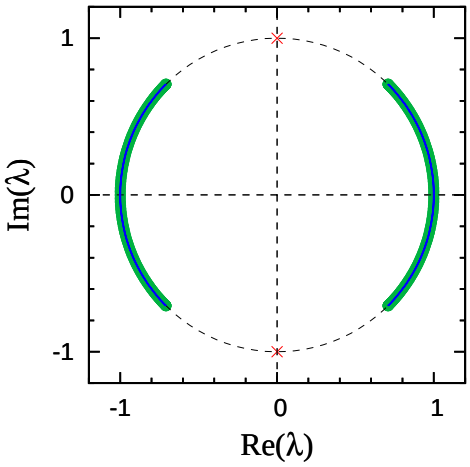

Fig. 5. ($\sigma_+ = 3\pi/2, \sigma_- = \pi/2$)
Green dense dots and red crosses : Numerically calculated eigenvalues λ of the time-evolution operator of the complete two-phase QW with chiral symmetry on the path.
Eigenvalues corresponding to the exponentially localized eigenvector are highlighted by red crosses.
Blue curves : The eigenvalues in Eq. (14).
The dashed curve represents a unit circle on the complex plane.

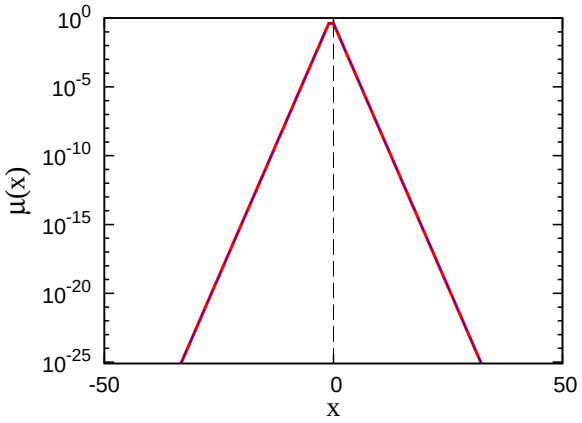

Fig. 6. ($\sigma_+ = 3\pi/2, \sigma_- = \pi/2$)
Red solid line : Probability distribution of the numerically calculated eigenvector with the eigenvalue $\lambda = i$.
Blue dashed line : The stationary measure in Eq. (24) with the normalization constant $c^2 = 1/(4+3\sqrt{2})$.

and that for $\lambda^{(3)}$ and $\lambda^{(4)}$ by

$$\mu(x) = \begin{cases} \frac{c^2}{2}(3+\sqrt{3})\left(\frac{1}{2+\sqrt{3}}\right)^x & (x \geq 1) \\ \frac{c^2}{2}(3+\sqrt{3}) & (x = 0) \\ \frac{c^2}{2}(9+5\sqrt{3})\left(\frac{1}{2+\sqrt{3}}\right)^{|x|} & (x \leq -1) \end{cases}$$
$$= \begin{cases} \frac{c^2}{2}(3+\sqrt{3})\left(\frac{1}{2+\sqrt{3}}\right)^x & (x \geq 0) \\ \frac{c^2}{2}(3+\sqrt{3})\left(\frac{1}{2+\sqrt{3}}\right)^{|x|-1} & (x \leq -1) \end{cases} . \quad (34)$$

2. Case of $\sqrt{q} = \sqrt{-6i} = -\sqrt{3}(1-i)$:
We obtain the eigenvalues

$$\lambda^{(1)} = \sqrt{-\frac{1}{2} + \frac{\sqrt{3}}{2}i}, \qquad \lambda^{(2)} = -\lambda^{(1)},$$

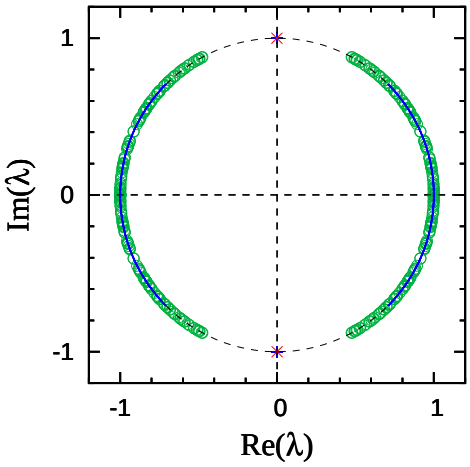

Fig. 7. ($\sigma_+ = 3\pi/2, \sigma_- = \pi/2$)
Green open dots and red crosses: Numerically calculated eigenvalue λ of the time-evolution operator of the complete two-phase QW with the perturbative coin on the path.
Blue curves : The eigenvalues in Eq. (14).

and

$$\lambda^{(3)} = \sqrt{-\frac{1}{2} - \frac{\sqrt{3}}{2}i}, \qquad \lambda^{(4)} = -\lambda^{(3)}.$$

The eigenvalues $\lambda^{(1)}$ and $\lambda^{(2)}$ in this case, thereby, are the same with $\lambda^{(3)}$ and $\lambda^{(4)}$ under the case 1. in Eq. (32), respectively, and vice verse. In the same way, the stationary measure for $\lambda^{(1)}$ and $\lambda^{(2)}$ is given by Eq. (34), and that for $\lambda^{(3)}$ and $\lambda^{(4)}$ is given by Eq. (33).

The fact that the all eigenvalues derived from Theorem 1 deviate from $\lambda = \pm i$ is consistent with the result by the bulk-edge correspondence. The stationary measure in Eq. (33) exponentially diverges as $|x|$ approaches to infinity, while that in Eq. (34) shows the exponential decay from the origin, thus, localization. However, this localization cannot be related to the topological invariant, and then the novel topological protection under perturbations is never expected. By the way, we see by Eq. (34) that the stationary distribution without the relevant symmetry has also symmetry around $x = -1/2$, which is identical with that of the stationary measure with chiral symmetry.

Then, we focus on the time-averaged limit measure. Let the initial coin state be $\varphi_0 = {}^T[1, 0]$. Theorem 2 gives the time-averaged limit measure of the complete two-phase QW without the relevant symmetries by

$$\overline{\mu}_\infty(x) = \begin{cases} \dfrac{(3+\sqrt{3})}{6(2+\sqrt{3})^{x+2}} & (x \geq 1) \\ \dfrac{(3+\sqrt{3})}{6(2+\sqrt{3})^{2}} & (x = 0) \\ \dfrac{(3+\sqrt{3})}{6(2+\sqrt{3})^{|x|+1}} & (x \leq -1) \end{cases}$$

$$= \begin{cases} \dfrac{(3+\sqrt{3})}{6(2+\sqrt{3})^{x+2}} & (x \geq 0) \\ \dfrac{(3+\sqrt{3})}{6(2+\sqrt{3})^{|x|+1}} & (x \leq -1) \end{cases}. \tag{35}$$

We remark that the above time-averaged limit measure agrees with the stationary measure in Eq. (34) by putting

$$c^2 = \frac{1}{3(2+\sqrt{3})^2}.$$

From this point of view, the stationary measure exhibiting the divergence at infinity is excluded. Here we get the coefficient of the delta function by

$$C = \sum_x \overline{\mu}_\infty(x) = 0.154701... > 0.$$

According to Theorem 3, the weight function is given by

$$w(x) = \begin{cases} \dfrac{2x^2(3-x)}{x^2+1} & (x \geq 0), \\ \dfrac{2x^2(1-x)}{x^2+1} & (x < 0). \end{cases}$$

Hence we see

$$\int_{-\frac{1}{\sqrt{2}}}^{\frac{1}{\sqrt{2}}} w(x) f_K(x; 1/\sqrt{2}) dx = 0.845299.... \tag{36}$$

Therefore we have

$$C + \int_{-\frac{1}{\sqrt{2}}}^{\frac{1}{\sqrt{2}}} w(x) f_K(x; 1/\sqrt{2}) dx = 1.$$

Here we present the numerical results of the time-averaged limit measure in Fig. 8 and the probability distribution at time 10000 in re-scaled space $(x/10000, 10000 P_{10000}(x))$ in Fig. 9. The observed behaviors are consistent with those in the previous subsection for the complete two-phase QW with chiral symmetry.

Again, we numerically calculate the eigenvalue of the two-phase QW with the coin operator in Eq. (31) on the path in the range of $-N \leq x \leq N-1$ with $N = 100$. As shown in Fig. 10, we confirm that densely distributed

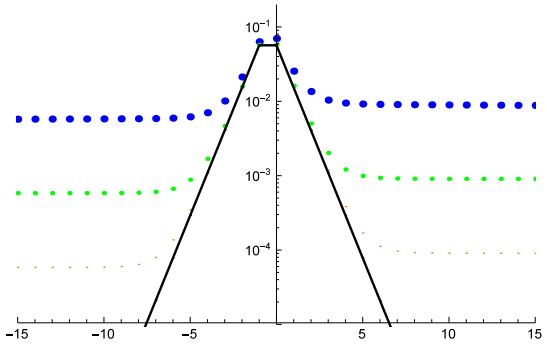

Fig. 8. ($\sigma_+ = \pi, \sigma_- = \pi/2$, ${}^T[\alpha, \beta] = {}^T[1, 0]$)
Black line: the time-averaged limit measure,
Blue dotted line: time-averaged probability till time 100,
Green dotted line:time-averaged probability till time 1000,
Orange dotted line: time-averaged probability till time 10000 .

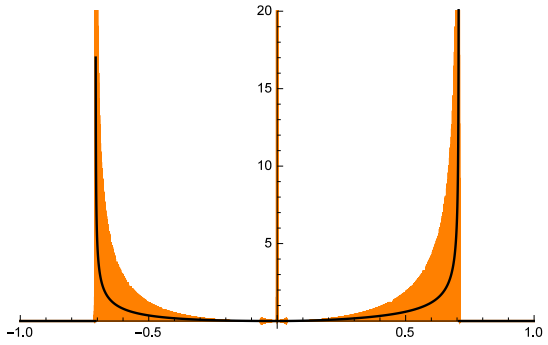

Fig. 9. ($\sigma_+ = \pi, \sigma_- = \pi/2$, ${}^T[\alpha, \beta] = {}^T[1, 0]$)
Orange curve: Probability distribution in a re-scaled space $(x/10000, 10000 P_{10000}(x))$ at time 10000,
Black curve: $w(x) f_K(x; 1/\sqrt{2})$.

eigenvalues are consistent with Eq. (14) and there exist two isolated eigenvalues at $\lambda \neq \pm i$. These isolated eigenvalues seem to be consistent with two of four eigenvalues derived by Theorem 1. The other two eigenvalues from Theorem 1 correspond to the unphysical solutions due to the divergence of the stationary measure. We also check that the probability distribution calculated from the isolated eigenvector on the upper half plane is exponentially localized and its exponential decay rate is consistent with that of the stationary measure in Eq. (34).

Finally, we check robustness of these localized states against the perturbative coin operator U_p. We employ the same condition with the previous subsection, except for the value of σ_+. Figure 12 shows the eigenvalue of the two-phase QW with the above perturbative coin on the path. We clearly see that all eigenvalues even corresponding to localization changes their values under the perturbation, in contrast to the previous case. Taking account of the above observations, we concluded that the two-phase QW with $\sigma_+ = \pi$ and $\sigma_- = \pi/2$ does have the localized eigenvectors, while they do not originate to the topological invariant.

4.4 localization length

In the previous subsections, we showed three examples with different phase parameter sets of σ_+ and σ_- of the complete two-phase QW. Here we show how localization depends on the phase relative difference $\sigma = (\sigma_+ - \sigma_-)/2$. To this end, we simplify the time-averaged limit measure of the complete two-phase QW in Theorem 2. Taking into account the fact that the time-averaged limit measure depends only on the relativistic value of the phase parameters $\sigma = (\sigma_+ - \sigma_-)/2$ with the initial coin state $\varphi_0 = {}^T[1, 0]$, we obtain the simplified exponential form up to the prefactors (which are slightly different in positive and negative regions and at the origin):

$$\overline{\mu}_\infty(x) \propto \exp\left(-\frac{2|x|}{\xi(\sigma)}\right), \tag{37}$$

$$\xi(\sigma)^{-1} = \ln\left\{3 - 2\sqrt{2}a(\sigma)\right\}/2, \tag{38}$$

$$a(\sigma) = \cos\{|\varphi(\sigma)| + |\sigma|\}, \quad \cos\varphi(\sigma) = \frac{1}{\sqrt{2}}\cos(\sigma),$$

where $\xi(\sigma)$ is called *the localization length* as the terminology in physics. Figure 13 shows the relative phase difference σ dependence on the localization length $\xi(\sigma)$. We remark that the localization length becomes minimum

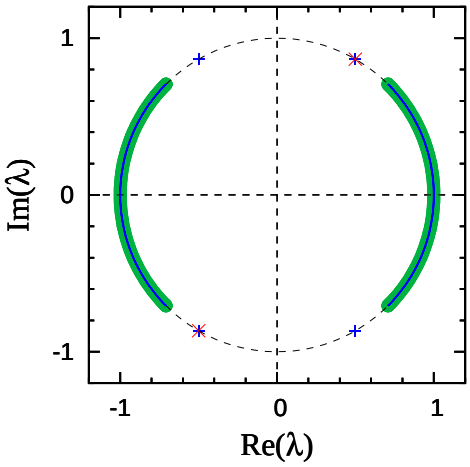

Fig. 10. ($\sigma_+ = \pi, \sigma_- = \pi/2$)
Green dense dots and red crosses : Numerically calculated eigenvalues λ of the time-evolution operator of the complete two-phase QW without the relevant symmetries for topological phases on the path. Eigenvalues corresponding to the exponentially localized eigenvector are highlighted by red crosses.
Blue curves : The eigenvalues in Eq. (14).
Blue crosses : The eigenvalues derived by Theorem 1.
The dashed curve represents a unit circle on the complex plane.

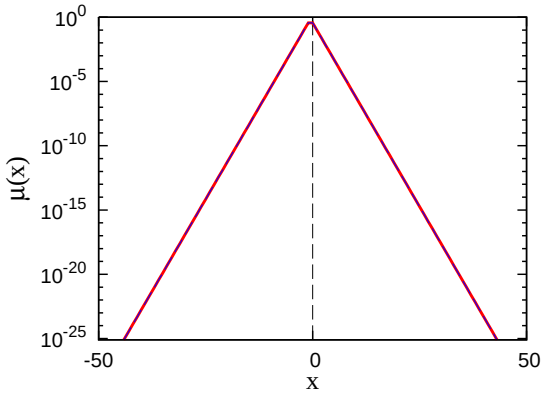

Fig. 11. ($\sigma_+ = \pi, \sigma_- = \pi/2$)
Red solid line : Probability distribution of the numerically calculated eigenvector showing localization on the upper half plane.
Blue dashed line : The stationary measure in Eq. (34) with the normalization constant $c^2 = (1+\sqrt{3})/(9+5\sqrt{3})$.

at $\sigma = \pm\pi/2$, and grows rapidly as σ goes to zero or π. At $\sigma = 0$ and π corresponding to the homogeneous QW, the localization length $\xi(\sigma)$ diverges, which indicates the vanishing of localization.

4.5 relation to the two-phase QW with one defect

Finally, we mention the relation between the complete two-phase QW and the two-phase QW with one defect studied in [13, 14]. The two-phase QW with one defect is characterized by the following coin operator

$$U'_x = \begin{cases} \frac{1}{\sqrt{2}} \begin{bmatrix} 1 & e^{i\sigma_+} \\ e^{-i\sigma_+} & -1 \end{bmatrix} & (x \geq 1) \\ \begin{bmatrix} 1 & 0 \\ 0 & -1 \end{bmatrix} & (x = 0) \\ \frac{1}{\sqrt{2}} \begin{bmatrix} 1 & e^{i\sigma_-} \\ e^{-i\sigma_-} & -1 \end{bmatrix} & (x \leq -1) \end{cases}, \tag{39}$$

with $\sigma_\pm \in [0, 2\pi)$. Only the difference from the complete two-phase QW is the coin at the origin ($x = 0$). The eigenvalue problem of the unitary matrix $U^{(s)} = SU'_x$ is studied in Ref. [13], and four eigenvalues are derived

$$\lambda^{(1)} = -\lambda^{(2)} = \frac{\cos\sigma + (\sin\sigma + \sqrt{2})i}{\sqrt{3 + 2\sqrt{2}\sin\sigma}}, \quad \lambda^{(3)} = -\lambda^{(4)} = \frac{\cos\sigma + (\sin\sigma - \sqrt{2})i}{\sqrt{3 - 2\sqrt{2}\sin\sigma}},$$

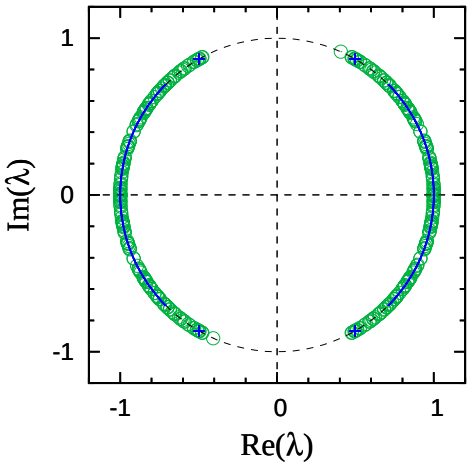

Fig. 12. ($\sigma_+ = \pi, \sigma_- = \pi/2$)
Green open dots and red crosses: Numerically calculated eigenvalue λ of the time-evolution operator of the complete two-phase QW with the perturbative coin on the path.
Blue curves : eigenvalues in Eq. (14).
Blue crosses : eigenvalues derived by Theorem 1.

with the relative phase difference $\sigma = (\sigma_+ - \sigma_-)/2$. The corresponding stationary measure is also derived in Ref. [13] and summarized as follows: The stationary measure obtained from the eigenvectors of $\lambda^{(1)}$ and $\lambda^{(2)}$ is derived as

$$\mu(x) = \begin{cases} c^2(2+\sqrt{2}\sin\sigma)\left(\dfrac{1}{3+2\sqrt{2}\sin\sigma}\right)^x & (x \geq 1) \\ c^2 & (x = 1) \\ c^2\left\{2+\sqrt{2}\sin\left(\dfrac{\sigma_+ + 3\sigma_-}{2}\right)\right\}\left(\dfrac{1}{3+2\sqrt{2}\sin\sigma}\right)^{|x|} & (x \leq -1) \end{cases} \tag{40}$$

and that from the eigenvectors of $\lambda^{(3)}$ and $\lambda^{(4)}$ becomes

$$\mu(x) = \begin{cases} c^2(2-\sqrt{2}\sin\sigma)\left(\dfrac{1}{3-2\sqrt{2}\sin\sigma}\right)^x & (x \geq 1) \\ c^2 & (x = 1) \\ c^2\left\{2-\sqrt{2}\sin\left(\dfrac{\sigma_+ + 3\sigma_-}{2}\right)\right\}\left(\dfrac{1}{3-2\sqrt{2}\sin\sigma}\right)^{|x|} & (x \leq -1) \end{cases} \tag{41}$$

When $\sigma = \pm\pi/2$, we find double-degenerated eigenvalues $\lambda^{(1)} = \lambda^{(3)} = \pm i$ and $\lambda^{(2)} = \lambda^{(4)} = \mp i$. By looking the stationary measures, in this case, we distinguish them by the decay rate, that is, the exponentially decay or divergence from the origin. If $\sigma \neq \pm\pi/2$, we have non-degenerated eigenvalues at $\lambda \neq \pm i$. These observations

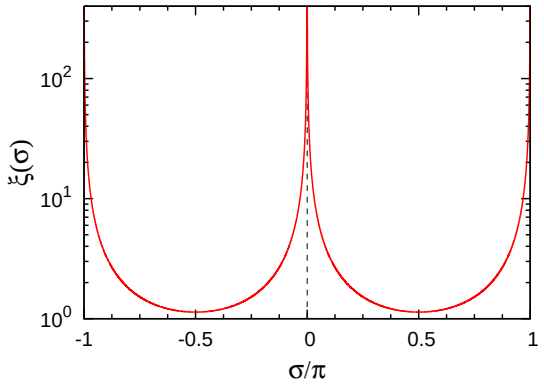

Fig. 13. The phase relativistic value σ dependence on the localization length $\xi(\sigma)$. Note the relation $\xi(-\sigma) = \xi(\sigma)$.

are the same with that of the complete two-phase QW as we see in the previous subsections. Furthermore, when $\sigma = \pm\pi/2$, which corresponds to the chiral symmetry, we emphasize that the decay rate of the stationary measure for the complete two-phase QW agrees with that of the two-phase QW with one defect. Thereby, this gives a hint to find the relation between the two inhomogeneous QWs.

Then, we need to understand how the coin operator at $x = 0$ of the two-phase QW with one defect, say the defect coin operator, affects on the localized states. We can confirm that the defect coin operator satisfies Eq. (18), indicating that the defect coin operator is identical with the perturbative coin U_p with $\theta_x = 0$. Assuming that the defect coin operator replaces the coin operator at a certain position x of the complete two-phase QW with the relevant symmetries for topological phases ($\sigma = \pm\pi/2$), this is nothing but the symmetry preserving perturbation. Therefore, the localized states of the two-phase QW with one defect can be regarded as the localized states of the complete two-phase QW survived from the symmetry preserving perturbation at the origin.

5 Summary

In this paper, we treated the complete two-phase QW, which can be considered as an ideal mathematical model of topological insulator. We obtained a measure and two kinds of limit theorems describing localization and the ballistic behavior. Indeed, we got the stationary and time-averaged limit measures for our QW at first. We gave a suggestion that localization can be occurred independently of the phases of the time-evolution operators and initial state of the walker, unless the two phases are the same. In addition, owing to the asymmetric unitary matrices, both the stationary and time-averaged limit measures are generally asymmetric for the origin, however, the stationary and time-averaged measures become symmetric at $x = -1/2$ at least, for the two cases studied in Section 4. This indicates that the defect at the origin of the two-phase QW with one defect makes the time-averaged distribution symmetric at the origin[13]. Moreover, we presented the weak convergence theorem which describes the ballistic behavior in the probability distributions for the position of the walker in re-scaled spaces. We also studied the topological invariant of the complete two-phase QW. We clarified that the time-evolution operator of the complete two-phase QW possesses chiral symmetry with $\varepsilon_\Gamma = -\pi/2$, when the two phases satisfy $\sigma_+ - \sigma_- = n\pi$ ($n \in \mathbb{Z}$). Therefore, the complete two-phase QW belongs to class AIII in the Cartan classification. Then, we derived the topological numbers for two-specific eigen values $\lambda = \pm i$. Taking into account these results, we compared the mathematical rigorous results with prediction by the bulk-edge correspondence, and confirmed the perfect agreements. Furthermore, we succeeded to find the relation between localization of the two-phase QW

with one defect and one of the complete two-phase QW, by considering that the defect coin operator at the origin as the symmetry preserving perturbation on the complete two-phase QW. In addition, we succeeded to relate the stationary and time-averaged limit measures by using both mathematical and physical consideration, which indicates that we can analyze localization of QWs by the stationary measure. The approach used in the present work would provide solid arguments to understand localization of various QWs in term of topological invariant.

Acknowledgments

TE is supported by Toshiko Yuasa Memorial Scholarship Fund. NK acknowledges financial support of the Grant-in-Aid for Scientific Research (C) of Japan Society for the Promotion of Science (No.21540116). HO is supported by Grant-in-Aid (Nos. 25800213 and 25390113) from the Japan Society for Promotion of Science.

References

1. A. Ahlbrecht, V. B. Scholz, and A. H. Werner: Disordered quantum walks in one lattice dimension, Journal of Mathematical Physics **52**, 102201 (2011)
2. J. K. Asbóth: Symmetries, topological phases, and bound states in the one-dimensional quantum walk, Physical Review B **86**, 195414 (2012)
3. J. K. Asbóth and J. M. Edge: Edge-state-enhanced transport in a two-dimensional quantum walk, Physical Review A **91**, 022324 (2015)
4. J.K. Asboth and H. Obuse: Bulk-boundary correspondence for chiral symmetric quantum walks, Physical Review B **88**, 121406(R) (2013)
5. A. B. Bernevig and T. L. Hughes: Topological Insulators and Topological Supercnductors, Princeton University Press, Princeton, NJ (2013)
6. M. J. Cantero, F. A. Grunbaum, L. Moral, and L. Velazquez: One-dimensional quantum walks with one defect, World Scientific **24**, 1250002 (2012)
7. C. Cedsich, F. A. Grünbaum, C. Stahl, L. Velázquez, A. H. Werner, and R. F. Werner: Bulk-edge correspondence of one-dimensional quantum walks, arXiv:1502.0259.
8. C. M. Chandrashekar, H. Obuse, and Th. Busch: Entanglement Properties of Localized States in 1D Topological Quantum Walks, arXiv:1502.00436.
9. K. Chisaki, M. Hamada, N. Konno, and E. Segawa: Limit theorems for discrete-time quantum walks on trees, Interdisciplinary Information Sciences **15**, 423-429 (2009)
10. C.-K. Chiu, J. C. Y. Teo, A. P. Schnyder, and S. Ryu: Classification of topological quantum matter with symmetries, arXiv:1505.03535.
11. A. Crespi, R. Osellame, R. Ramponi, V. Giovannetti, R. Fazio, L. Sansoni, F. D. Nicola, F. Sciarrino, and P. Mataloni: Anderson localization of entangled photons in an integrated quantum walk, Nature Potonics **7**, 322 (2013)
12. J. M. Edge and J. K. Asbóth: Localization, delocalization, and topological transitions in disordered two-dimensional quantum walks, Physical Review B **91**, 104202 (2015)
13. S. Endo, T. Endo, N. Konno, E. Segawa, and M. Takei: Limit theorems of a two-phase quantum walk with one-defect, Quantum Information and Computation **15**, 1373-1396 (2015)
14. S. Endo, T. Endo, N. Konno, E. Segawa, and M. Takei: Weak limit theorem of a two-phase quantum walk with one defect, arXiv:1412.4309
15. T. Endo and N. Konno: The stationary measure of a space-inhomogeneous quantum walk on the line, Yokohama Mathematical Journal **60**, 33-47 (2014)
16. T. Endo and N. Konno: The time-averaged limit measure of the Wojcik model, Quantum Information and Computation **15**, 0105-0133 (2015)
17. T. Endo and N. Konno: Weak convergence of the Wojcik model, arXiv:1412.7874.
18. T. Endo, N. Konno, E. Segawa, and M. Takei: A one-dimensional Hadamard walk with one defect, Yokohama Mathematical Journal **60**, 49-90 (2014)
19. G. Grimmett, S. Janson, and P. F. Scudo: weak convergences for quantum random walks, Physical Review E **69**, 026119 (2004)
20. M. Z. Hasan and C. L. Kane: *Colloquium* : Topological insulators, Reviews of Modern Physics **82**, 3045-3067 (2010)

21. Y. Ide and N. Konno: Continuous-time quantum walks on the threshold network model, Mathematical Structures in Computer Science **20**, 1079-1090 (2010)
22. Y. Ide, N. Konno, and E. Segawa: Time averaged distribution of a discrete-time quantum walk on the path: Quantum Information Processing **11**, 1207-1218 (2012).
23. N. Inui, Y. Konishi, and N. Konno: Localization of two-dimensional quantum walks, Physical Review A **69**, 052323 (2003)
24. A. Joye and M. Merkli: Dynamical localization of quantum walks in random environments, Journal of Statistical Physics **140**, 1025-1053 (2010)
25. T. Kitagawa: Topological phenomena in quantum walks; elementary introduction to the physics of topological phases, Quantum Information Processing **11**, 1107-1148 (2012)
26. T. Kitagawa, E. Berg, M. Rudner, and E. Demler: Topological characterization of periodically driven quantum systems: Physical Review B **83**, 235114 (2010).
27. T. Kitagawa, M. A. Broome, A. Fedrizzi, M. S. Rudner, E. Berg, I. Kassal, A. Aspuru-Guzik, E. Demler, and A. G. White: Observation of topologically protected bound states in a one dimensional photonic system, Nature Communications **3**, 882 (2012)
28. T. Kitagawa, M. S. Rudner, E. Berg, and E. Demler: Exploring topological phases with quantum walks, Physical Review A **82**, 033429 (2010)
29. N. Konno: A New Type of Limit Theorems for the One-dimensional quantum random walk, Journal of the Mathematical Society of Japan **57**, 1179-1195 (2005)
30. N. Konno: A path integral approach for disordered quantum walks in one dimension, Fluctuation and Noise Letters, **5**, 529-537 (2005)
31. N. Konno, T. Luczak, and E. Segawa: Limit measures of inhomogeneous discrete-time quantum walks in one dimension, Quantum Information Processing **12**, 33-53 (2013)
32. N. H. Lindner, G. Refael, and V. Galitski: Floquet topological insulator in semiconductor quantum wells: Nature Physics **7**, 490495 (2011).
33. A. Nayak and A. Vishwanath: Quantum walk on the line, arXiv:quant-ph/0010117
34. M. Mohseni, P. Rebentrost, S. Lloyd, A. Aspuru-Guzik: Environment-Assisted Quantum Walks in Photosynthetic Energy Transfer, Journal of Chemical Physics **129**, 174106 (2008)
35. H. Obuse, J. K. Asbóth, Y. Nishimura, and N. Kawakami: Unveiling hidden topological phases of a one-dimensional Hadamard quantum walk, Physical Review B **92**, 045424 (2015).
36. H. Obuse and N. Kawakami: Topological phases and delocalization of quantum walks in random environments, Physical Review B **84**, 195139 (2011)
37. X.-L. Qi and S.-C. Zhang: Topological insulators and superconductors, Reviews of Modern Physics **83**, 1057-1110 (2011)
38. T. Rakovszky and J. K. Asbóth: Localization, delocalization, and topological phase transitions in the one-dimensional split-step quantum walk: arXiv:1505.04513 (2015).
39. A. P. Schnyder, S. Ryu, A. Furusaki, and A. W. W. Ludwig: Classification of topological insulators and superconductors in three spatial dimensions, Physical Review B **78**, 195125 (2008).
40. A. Schreiber, K. N. Cassemiro, V. Potocek, A. Gábris, I. Jex, and Ch. Silberhorn: Decoherence and Disorder in Quantum Walks: From Ballistic Spread to Localization: Physical Review Letter **106**, 180403 (2011)
41. B. Tarasinski, J. K. Asbóth, and J. P. Dahlhaus: Scattering theory of topological phases in discrete-time quantum walks Physical Review A **89**, 042327 (2014)
42. A. Wojcik, T. Luczak, P. Kurzynski, A. Grudka, T. Gdala, and M. Bednarska-Bzdega: Trapping a particle of a quantum walk on the line, Physical Review A **85**, 012329 (2012)

Appendix A

In Appendix A, we give the detail of the derivation of Theorem 1. Throughout Appendix A, let us focus on the eigenvalue problem

$$U^{(s)}\Psi = \lambda\Psi, \tag{A.1}$$

where $\lambda \in \mathbb{C}$ with $|\lambda| = 1$, and $\Psi \in (\mathbb{C}^2)^\infty$. Taking advantage of the SGF method[15], we solve the eigenvalue

problem (A.1). We can rewrite the eigenvalue problem for position $x \in \mathbb{Z}$ by

$$\lambda\Psi(x) = P_{x+1}\Psi(x+1) + Q_{x-1}\Psi(x-1). \tag{A.2}$$

Now Eq. (A.2) can be written depending on the position in the following way:

1. Case of $x = 1, 2, 3, \cdots$:

$$\lambda\Psi^L(x) = \frac{1}{\sqrt{2}}\Psi^L(x+1) + \frac{e^{i\sigma_+}}{\sqrt{2}}\Psi^R(x+1), \tag{A.3}$$

$$\lambda\Psi^R(x) = \frac{e^{-i\sigma_+}}{\sqrt{2}}\Psi^L(x-1) - \frac{1}{\sqrt{2}}\Psi^R(x-1). \tag{A.4}$$

2. Case of $x = -2, -3, -4, \cdots$:

$$\lambda\Psi^L(x) = \frac{1}{\sqrt{2}}\Psi^L(x+1) + \frac{e^{i\sigma_-}}{\sqrt{2}}\Psi^R(x+1), \tag{A.5}$$

$$\lambda\Psi^R(x) = \frac{e^{-i\sigma_-}}{\sqrt{2}}\Psi^L(x-1) - \frac{1}{\sqrt{2}}\Psi^R(x-1). \tag{A.6}$$

3. Case of $x = -1$ case:

$$\lambda\Psi^L(-1) = \frac{1}{\sqrt{2}}\Psi^L(0) + \frac{e^{i\sigma_+}}{\sqrt{2}}\Psi^R(0), \tag{A.7}$$

$$\lambda\Psi^R(-1) = \frac{e^{-i\sigma_-}}{\sqrt{2}}\Psi^L(-2) - \frac{1}{\sqrt{2}}\Psi^R(-2). \tag{A.8}$$

4. Case of $x = 0$:

$$\lambda\Psi^L(0) = \frac{1}{\sqrt{2}}\Psi^L(1) + \frac{e^{i\sigma_+}}{\sqrt{2}}\Psi^R(1), \tag{A.9}$$

$$\lambda\Psi^R(0) = \frac{e^{-i\sigma_-}}{\sqrt{2}}\Psi^L(-1) - \frac{1}{\sqrt{2}}\Psi^R(-1). \tag{A.10}$$

Next, we introduce the generating functions of $\Psi^j(x)$ $(j = L, R)$:

$$f_+^j(z) = \sum_{x=1}^{\infty}\Psi^j(x)z^x, \quad f_-^j(z) = \sum_{x=-1}^{-\infty}\Psi^j(x)z^x, \tag{A.11}$$

which provide

Lemma A.1 *Put*

$$A = \begin{bmatrix} \lambda - \dfrac{1}{\sqrt{2}z} & -\dfrac{e^{i\sigma_\pm}}{\sqrt{2}z} \\ -\dfrac{e^{-i\sigma_\pm}}{\sqrt{2}}z & \lambda + \dfrac{z}{\sqrt{2}} \end{bmatrix},\ \mathbf{f}_\pm(z) = \begin{bmatrix} f_\pm^L(z) \\ f_\pm^R(z) \end{bmatrix},$$

$$\mathbf{a}_+(z) = \begin{bmatrix} -\lambda\alpha \\ \left(\dfrac{e^{-i\sigma_+}}{\sqrt{2}}\alpha - \dfrac{1}{\sqrt{2}}\beta\right) z \end{bmatrix},\ \mathbf{a}_-(z) = \begin{bmatrix} \left(\dfrac{1}{\sqrt{2}}\alpha + \dfrac{e^{i\sigma_+}}{\sqrt{2}}\beta\right) z^{-1} \\ -\lambda\beta \end{bmatrix},$$

with $\alpha = \Psi^L(0)$ *and* $\beta = \Psi^R(0)$.

Then,

$$A_\pm \mathbf{f}_\pm(z) = \mathbf{a}_\pm(z) \tag{A.12}$$

holds.

Taking account of

$$\det A_\pm = \frac{\lambda}{\sqrt{2}z}\left\{z^2 - \sqrt{2}\left(\frac{1}{\lambda} - \lambda\right)z - 1\right\}, \tag{A.13}$$

we put θ_s, $\theta_l \in \mathbb{C}$ satisfying

$$\det A_\pm = \frac{\lambda}{\sqrt{2}z}(z - \theta_s)(z - \theta_l) \tag{A.14}$$

and $|\theta_s| \leq 1 \leq |\theta_l|$. By Eqs. (A.13) and (A.14), we see $\theta_s\theta_l = -1$.
Hereafter let us derive $f_\pm^L(z)$ and $f_\pm^R(z)$ from Lemma A.1.

1. Case of $f_+^L(z)$: Eq. (A.12) gives

$$f_+^L(z) = -\frac{\alpha z}{(z - \theta_s)(z - \theta_l)}\left\{z - \left(\frac{1}{\sqrt{2}\lambda} - \frac{e^{i\sigma_+}\beta}{\sqrt{2}\lambda\alpha} - \sqrt{2}\lambda\right)\right\}.$$

Putting $\theta_s = \dfrac{1}{\sqrt{2}\lambda} - \dfrac{e^{i\sigma_+}\beta}{\sqrt{2}\lambda\alpha} - \sqrt{2}\lambda$, we have

$$\begin{aligned} f_+^L(z) &= -\frac{\alpha z}{z - \theta_l} = -\frac{\alpha z}{z + \dfrac{1}{\theta_s}} = -\frac{\alpha z\theta_s}{1 + \theta_s z} \\ &= -\alpha(\theta_s z)\left\{1 + (-\theta_s z) + (-\theta_s z)^2 + (-\theta_s z)^3 + \cdots\right\}. \end{aligned}$$

Hence we see

$$f_+^L(z) = \alpha\sum_{x=1}^{\infty}(-\theta_s z)^x. \tag{A.15}$$

Equation (A.15) and the definition of $f_+^L(z)$ give

$$\Psi^L(x) = \alpha(-\theta_s)^x \quad (x = 1, 2, \cdots), \tag{A.16}$$

where

$$\theta_s = \frac{1}{\sqrt{2}\lambda} - \frac{e^{i\sigma_+}\beta}{\sqrt{2}\lambda\alpha} - \sqrt{2}\lambda. \tag{A.17}$$

2. Case of $f_+^R(z)$: Putting $\theta_s = \dfrac{1}{\sqrt{2}\lambda} - \dfrac{e^{-i\sigma_+}\alpha}{\sqrt{2}\lambda\beta}$, we have from Eq. (A.12)

$$\begin{aligned} f_+^R(z) &= \frac{\beta\theta_l^{-1}z}{1-\theta_l^{-1}z} \\ &= \beta\sum_{x=1}^{\infty}(-\theta_s z)^x. \end{aligned} \tag{A.18}$$

Equation (A.18) and the definition of $f_+^R(z)$ imply

$$\Psi^R(x) = \beta(-\theta_s)^x \quad (x = 1, 2, \cdots), \tag{A.19}$$

where

$$\theta_s = \frac{1}{\sqrt{2}\lambda} - \frac{e^{-i\sigma_+}\alpha}{\sqrt{2}\lambda\beta}. \tag{A.20}$$

3. Case of $f_-^L(z)$: Putting $\theta_s = \dfrac{\alpha + \beta e^{i\sigma_+}}{\sqrt{2}\lambda\left\{\alpha + \beta(e^{i\sigma_+} - e^{i\sigma_-})\right\}}$, Eq. (A.12) gives

$$\begin{aligned} f_-^L(z) &= \frac{\left\{\alpha + \beta(e^{i\sigma_+} - e^{i\sigma_-})\right\}\theta_s^{-1}\theta_l^{-1}z^{-1}}{z^{-1} - \theta_s^{-1}} \\ &= \frac{\left\{\alpha + \beta(e^{i\sigma_+} - e^{i\sigma_-})\right\}\theta_s z^{-1}}{1 - \theta_s z^{-1}} \\ &= \left\{\alpha + \beta(e^{i\sigma_+} - e^{i\sigma_-})\right\}\theta_s z^{-1}\left\{1 + \theta_s z^{-1} + (\theta_s z^{-1})^2 + (\theta_s z^{-1})^3 + \cdots\right\} \\ &= \sum_{x=-1}^{-\infty}\left\{\alpha + \beta(e^{i\sigma_+} - e^{i\sigma_-})\right\}\theta_s^{|x|}z^x. \end{aligned} \tag{A.21}$$

Equation (A.21) and the definition of $f_-^L(z)$ yield

$$\Psi^L(x) = \left\{\alpha + \beta(e^{i\sigma_+} - e^{i\sigma_-})\right\}\theta_s^{|x|} \quad (x = -1, -2, \cdots),$$

where

$$\theta_s = \frac{\alpha + \beta e^{i\sigma_+}}{\sqrt{2}\lambda\left\{\alpha + \beta(e^{i\sigma_+} - e^{i\sigma_-})\right\}}. \tag{A.22}$$

4. Case of $f_-^R(z)$: Putting $\theta_s = -\sqrt{2}\lambda + \dfrac{1}{\sqrt{2}e^{i\sigma_-}\lambda\beta}(\alpha + e^{i\sigma_+}\beta)$, Eq. (A.12) implies

$$f_-^R(z) = \beta \sum_{x=-1}^{-\infty} \theta_s^{|x|} z^x. \tag{A.23}$$

Therefore Eq. (A.23) and the definition of $f_-^R(z)$ give

$$\Psi^R(x) = \beta\theta_s^{|x|} \quad (x = -1, -2, \cdots),$$

where

$$\theta_s = -\sqrt{2}\lambda + \frac{1}{\sqrt{2}e^{i\sigma_-}\lambda\beta}(\alpha + e^{i\sigma_+}\beta). \tag{A.24}$$

Consequently, we obtain

$$\Psi(x) = \begin{cases} (-\theta_s)^x \begin{bmatrix} \alpha \\ \beta \end{bmatrix} & (x = 1, 2, \ldots), \\ \begin{bmatrix} \alpha \\ \beta \end{bmatrix} & (x = 0), \\ \theta_s^{|x|} \begin{bmatrix} \alpha + (e^{i\sigma_+} - e^{i\sigma_-})\beta \\ \beta \end{bmatrix} & (x = -1, -2, \ldots). \end{cases} \tag{A.25}$$

From the above discussion, we obtain Proposition 1, the solutions of the eigenvalue problem (A.1) as follows:

Proposition 1 *Let $\lambda^{(j)}$ be the eigenvalues of the unitary matrix $U^{(s)}$, and $\Psi^{(j)}(0)$ be the eigenvector at $x = 0$, with $j = 1, 2, 3, 4$. Putting*

$$\begin{cases} p = e^{i\sigma_+}(e^{-2i\sigma_-} - e^{-2i\sigma_+} - 4e^{-2i\tilde{\sigma}}) \\ q = e^{-2i\sigma_-} + e^{-2i\sigma_+} - 6e^{-2i\tilde{\sigma}} \\ r^{(\pm)} = e^{-i\sigma_+} \pm e^{-i\sigma_-} \end{cases},$$

where $\tilde{\sigma} = (\sigma_+ + \sigma_-)/2$ and $c \in \mathbb{R}_+$, we obtain the solutions of the eigenvalue problem (4) as follows:

1. For $\lambda^{(1)} = \sqrt{\dfrac{p + e^{i\sigma_+} r^{(-)} \sqrt{q}}{2(-r^{(-)} - \sqrt{q})}}$ *and* $\Psi^{(1)}(0) = {}^T[\alpha,\ \beta] = {}^T \dfrac{c}{\sqrt{2}} \left[1,\ \dfrac{1}{2}(r^{(-)} + \sqrt{q})\right]$, *we have*

$$\Psi^L(x) = \begin{cases} \dfrac{c}{\sqrt{2}} \left(\dfrac{r^{(+)} - \sqrt{q}}{\sqrt{-r^{(-)} - \sqrt{q}} \sqrt{p + e^{i\sigma_+} r^{(-)} \sqrt{q}}} \right)^x & (x \geq 1) \\ \dfrac{c}{\sqrt{2}} & (x = 0) \\ \dfrac{c}{2\sqrt{2}} \left\{ 2 + (e^{i\sigma_+} - e^{i\sigma_-})(r^{(-)} + \sqrt{q}) \right\} \left(- \dfrac{r^{(+)} - \sqrt{q}}{\sqrt{-r^{(-)} - \sqrt{q}} \sqrt{p + e^{i\sigma_+} r^{(-)} \sqrt{q}}} \right)^{|x|} & (x \leq -1) \end{cases},$$

$$\Psi^R(x) = \begin{cases} \dfrac{c}{2\sqrt{2}} (r^{(-)} + \sqrt{q}) \left(\dfrac{r^{(+)} - \sqrt{q}}{\sqrt{-r^{(-)} - \sqrt{q}} \sqrt{p + e^{i\sigma_+} r^{(-)} \sqrt{q}}} \right)^x & (x \geq 1) \\ \dfrac{c}{2\sqrt{2}} (r^{(-)} + \sqrt{q}) & (x = 0) \\ \dfrac{c}{2\sqrt{2}} (r^{(-)} + \sqrt{q}) \left(- \dfrac{r^{(+)} - \sqrt{q}}{\sqrt{-r^{(-)} - \sqrt{q}} \sqrt{p + e^{i\sigma_+} r^{(-)} \sqrt{q}}} \right)^{|x|} & (x \leq -1) \end{cases}.$$

2. For $\lambda^{(2)} = -\sqrt{\dfrac{p + e^{i\sigma_+} r^{(-)} \sqrt{q}}{2(-r^{(-)} - \sqrt{q})}}$ *and* $\Psi^{(2)}(0) = \Psi^{(1)}(0) = {}^T \dfrac{c}{\sqrt{2}} \left[1,\ \dfrac{1}{2}(r^{(-)} + \sqrt{q})\right]$, *we have*

$$\Psi^L(x) = \begin{cases} \dfrac{c}{\sqrt{2}} \left(- \dfrac{r^{(+)} - \sqrt{q}}{\sqrt{-r^{(-)} - \sqrt{q}} \sqrt{p + e^{i\sigma_+} r^{(-)} \sqrt{q}}} \right)^x & (x \geq 1) \\ \dfrac{c}{\sqrt{2}} & (x = 0) \\ \dfrac{c}{2\sqrt{2}} \left\{ 2 + (e^{i\sigma_+} - e^{i\sigma_-})(r^{(-)} + \sqrt{q}) \right\} \left(\dfrac{r^{(+)} - \sqrt{q}}{\sqrt{-r^{(-)} - \sqrt{q}} \sqrt{p + e^{i\sigma_+} r^{(-)} \sqrt{q}}} \right)^{|x|} & (x \leq -1) \end{cases},$$

$$\Psi^R(x) = \begin{cases} \dfrac{c}{2\sqrt{2}} (r^{(-)} + \sqrt{q}) \left(- \dfrac{r^{(+)} - \sqrt{q}}{\sqrt{-r^{(-)} - \sqrt{q}} \sqrt{p + e^{i\sigma_+} r^{(-)} \sqrt{q}}} \right)^x & (x \geq 1) \\ \dfrac{c}{2\sqrt{2}} (r^{(-)} + \sqrt{q}) & (x = 0) \\ \dfrac{c}{2\sqrt{2}} (r^{(-)} + \sqrt{q}) \left(\dfrac{r^{(+)} - \sqrt{q}}{\sqrt{-r^{(-)} - \sqrt{q}} \sqrt{p + e^{i\sigma_+} r^{(-)} \sqrt{q}}} \right)^{|x|} & (x \leq -1) \end{cases}.$$

3. For $\lambda^{(3)} = \sqrt{\dfrac{p - e^{i\sigma_+} r^{(-)} \sqrt{q}}{2(-r^{(-)} + \sqrt{q})}}$ *and* $\Psi^{(3)}(0) = {}^T[\alpha,\ \beta] = {}^T \dfrac{c}{\sqrt{2}} \left[1,\ \dfrac{1}{2}(r^{(-)} - \sqrt{q})\right]$*, we have*

$$\Psi^L(x) = \begin{cases} \dfrac{c}{\sqrt{2}} \left(\dfrac{r^{(+)} + \sqrt{q}}{\sqrt{-r^{(-)} + \sqrt{q}} \sqrt{p - e^{i\sigma_+} r^{(-)} \sqrt{q}}} \right)^x & (x \geq 1) \\ \dfrac{c}{\sqrt{2}} & (x = 0) \\ \dfrac{c}{2\sqrt{2}} \left\{ 2 + (e^{i\sigma_+} - e^{i\sigma_-})(r^{(-)} - \sqrt{q}) \right\} \left(- \dfrac{r^{(+)} + \sqrt{q}}{\sqrt{-r^{(-)} + \sqrt{q}} \sqrt{p - e^{i\sigma_+} r^{(-)} \sqrt{q}}} \right)^{|x|} & (x \leq -1) \end{cases},$$

$$\Psi^R(x) = \begin{cases} \dfrac{c}{2\sqrt{2}} (r^{(-)} - \sqrt{q}) \left(\dfrac{r^{(+)} + \sqrt{q}}{\sqrt{-r^{(-)} + \sqrt{q}} \sqrt{p - e^{i\sigma_+} r^{(-)} \sqrt{q}}} \right)^x & (x \geq 1) \\ \dfrac{c}{2\sqrt{2}} (r^{(-)} - \sqrt{q}) & (x = 0) \\ \dfrac{c}{2\sqrt{2}} (r^{(-)} - \sqrt{q}) \left(- \dfrac{r^{(+)} + \sqrt{q}}{\sqrt{-r^{(-)} + \sqrt{q}} \sqrt{p - e^{i\sigma_+} r^{(-)} \sqrt{q}}} \right)^{|x|} & (x \leq -1) \end{cases}.$$

4. For $\lambda^{(4)} = -\sqrt{\dfrac{p - e^{i\sigma_+} r^{(-)} \sqrt{q}}{2(-r^{(-)} + \sqrt{q})}}$ *and* $\Psi^{(4)}(0) = \Psi^{(3)}(0) = {}^T \dfrac{c}{\sqrt{2}} \left[1,\ \dfrac{1}{2}(r^{(-)} - \sqrt{q})\right]$*, we have*

$$\Psi^L(x) = \begin{cases} \dfrac{c}{\sqrt{2}} \left(- \dfrac{r^{(+)} + \sqrt{q}}{\sqrt{-r^{(-)} + \sqrt{q}} \sqrt{p - e^{i\sigma_+} r^{(-)} \sqrt{q}}} \right)^x & (x \geq 1) \\ \dfrac{c}{\sqrt{2}} & (x = 0) \\ \dfrac{c}{2\sqrt{2}} \left\{ 2 + (e^{i\sigma_+} - e^{i\sigma_-})(r^{(-)} - \sqrt{q}) \right\} \left(\dfrac{r^{(+)} + \sqrt{q}}{\sqrt{-r^{(-)} + \sqrt{q}} \sqrt{p - e^{i\sigma_+} r^{(-)} \sqrt{q}}} \right)^{|x|} & (x \leq -1) \end{cases},$$

$$\Psi^R(x) = \begin{cases} \dfrac{c}{2\sqrt{2}} (r^{(-)} - \sqrt{q}) \left(- \dfrac{r^{(+)} + \sqrt{q}}{\sqrt{-r^{(-)} + \sqrt{q}} \sqrt{p - e^{i\sigma_+} r^{(-)} \sqrt{q}}} \right)^x & (x \geq 1) \\ \dfrac{c}{2\sqrt{2}} (r^{(-)} - \sqrt{q}) & (x = 0) \\ \dfrac{c}{2\sqrt{2}} (r^{(-)} - \sqrt{q}) \left(\dfrac{r^{(+)} + \sqrt{q}}{\sqrt{-r^{(-)} + \sqrt{q}} \sqrt{p - e^{i\sigma_+} r^{(-)} \sqrt{q}}} \right)^{|x|} & (x \leq -1) \end{cases}.$$

Here, 4 expressions of θ_s, that is, Eqs. (A.17), (A.20), (A.22), and (A.24) provide

$$\begin{aligned} \theta_s &= \frac{\alpha - 2\lambda^2 \alpha - e^{i\sigma_+} \beta}{\sqrt{2}\lambda\alpha} = \frac{\beta - e^{-i\sigma_+} \alpha}{\sqrt{2}\lambda\beta} \\ &= \frac{\alpha + \beta e^{i\sigma_+}}{\sqrt{2}\lambda \left\{ \alpha + \beta (e^{i\sigma_+} - e^{i\sigma_-}) \right\}} = -\sqrt{2}\lambda + \frac{1}{\sqrt{2} e^{i\sigma_-} \lambda \beta} (\alpha + e^{i\sigma_+} \beta), \end{aligned}$$

which leads to the conditions of $\lambda^{(j)}$ and $\Psi^{(j)}(0)$ $(j=1,2)$ in Proposition 1 and Theorem 1. Noting that the stationary measure is defined by $\mu(x)=|\Psi^R(x)|^2+|\Psi^L(x)|^2$ $(x\in\mathbb{R})$, we arrive at Theorem 1.

Appendix B

Hereafter, we prove Theorem 2 along with the *time-space generating function method*[31]. The protocol is similar to that of Section 4 in Ref. [13]. To begin with, we give some notations. The coin operator U_x can be divided into two parts by

$$U_x = P_x + Q_x,$$

where

$$P_x = \begin{bmatrix} a_x & b_x \\ 0 & 0 \end{bmatrix}, \ Q_x = \begin{bmatrix} 0 & 0 \\ c_x & d_x \end{bmatrix}.$$

Here we introduce a notation of the weight of all the passages of the walker which moves to the left l times and to the right m times till time t as follows[31]:

$$\Xi_t(l,m) = \sum_{l_j,m_j} P_{x_{l1}}^{l_1} Q_{x_{m1}}^{m_1} P_{x_{l2}}^{l_2} Q_{x_{m_2}}^{m_2} \cdots P_{x_{lt}}^{l_t} Q_{x_{mt}}^{m_t},$$

with $l+m=t$, $-l+m=x$, $\sum_i l_i = l$, $\sum_j m_j = m$, and $\sum_{\gamma=l_i,m_j} |x_\gamma| = x$. We remark that the time-averaged limit measure can be written by the square norm of the residue of the generating function $\tilde{\Xi}_x(z) \equiv \sum_{t\geq 0} \Xi_t(x) z^t$, which leads us to complete the proof:

Proposition 2 [16] *We have*

$$\overline{\mu}_\infty(x) = \sum_{\theta_j^{(\pm)}} \left\| Res(\tilde{\Xi}_x(z) : z = e^{i\theta_j^{(\pm)}})\varphi_0 \right\|^2,$$

where $\{e^{i\theta_j^{(\pm)}}\}$ *is the set of the singular points of* $\tilde{\Xi}_x(z)$.

Now we give useful concrete formula of $\tilde{\Xi}_x(z)$, which plays an important role for the proof. The derivation of Lemma B.1 comes from Lemma 3.1 in Ref. [31]. In Appendix B, we assume that the walker starts at the origin with the initial coin state $\varphi_0 = {}^T[\alpha,\beta]$, where $\alpha,\beta\in\mathbb{C}$, and $|\alpha|^2+|\beta|^2=1$.

Lemma B.1 *1. If* $x=0$, *we have*

$$\tilde{\Xi}_0(z) = \frac{1}{1-\frac{e^{-i\sigma_+}}{\sqrt{2}}\tilde{f}_0^{(+)}(z) - \frac{e^{i\sigma_+}}{\sqrt{2}}\tilde{f}_0^{(-)}(z) + \tilde{f}_0^{(+)}(z)\tilde{f}_0^{(-)}(z)} \begin{bmatrix} 1-\frac{e^{i\sigma_+}}{\sqrt{2}} & -\frac{1}{\sqrt{2}}\tilde{f}_0^{(+)}(z) \\ \frac{1}{\sqrt{2}}\tilde{f}_0^{(-)}(z) & 1-\frac{e^{-i\sigma_+}}{\sqrt{2}}\tilde{f}_0^{(+)}(z) \end{bmatrix}.$$

2. If $|x|\geq 1$, *we have*

$$\tilde{\Xi}_x(z) = \begin{cases} (\tilde{\lambda}^{(+)}(z))^{x-1} \begin{bmatrix} \tilde{\lambda}^{(+)}(z)\tilde{f}_0^{(+)}(z) \\ z \end{bmatrix} \left[\frac{e^{-i\sigma_+}}{\sqrt{2}}, -\frac{1}{\sqrt{2}}\right] \tilde{\Xi}_0(z) & (x\geq 1), \\ (\tilde{\lambda}^{(-)}(z))^{|x|-1} \begin{bmatrix} z \\ \tilde{\lambda}^{(-)}(z)\tilde{f}_0^{(-)}(z) \end{bmatrix} \left[\frac{1}{\sqrt{2}}, \frac{e^{i\sigma_+}}{\sqrt{2}}\right] \tilde{\Xi}_0(z) & (x\leq -1), \end{cases}$$

with $\tilde{\lambda}^{(+)}(z) = \dfrac{z}{e^{-i\sigma_+}\tilde{f}_0^{(+)}(z) - \sqrt{2}}$ *and* $\tilde{\lambda}^{(-)}(z) = \dfrac{z}{\sqrt{2} - e^{i\sigma_-}\tilde{f}_0^{(-)}(z)}$. *Note that* $\tilde{f}_0^{(+)}(z)$ *and* $\tilde{f}_0^{(-)}(z)$ *satisfy*

$$\begin{cases} (\tilde{f}_0^{(+)}(z))^2 - \sqrt{2}e^{i\sigma_+}(1+z^2)\tilde{f}_0^{(+)}(z) + e^{2i\sigma_+}z^2 = 0, \\ (\tilde{f}_0^{(-)}(z))^2 - \sqrt{2}e^{-i\sigma_-}(1+z^2)\tilde{f}_0^{(-)}(z) + e^{-2i\sigma_-}z^2 = 0. \end{cases}$$

Thereby, we obtain

Lemma B.2 $\tilde{f}_0^{(+)}(z)$ *and* $\tilde{f}_0^{(-)}(z)$ *are written down with respect to* θ *as*

$$\tilde{f}_0^{(\pm)}(z) = e^{i(\theta \pm \sigma_\pm)} \times e^{i\tilde{\phi}(\theta)}, \tag{B.1}$$

with

$$\sin\tilde{\phi}(\theta) = \mathrm{sgn}(\sin\theta)\sqrt{2\sin\theta^2 - 1}, \quad \cos\tilde{\phi}(\theta) = \sqrt{2}\cos\theta. \tag{B.2}$$

The derivation of Lemma B.2 is similar to Lemma 3 in Ref. [14], and we omit it here. By taking advantage of Lemmas B.1 and B.2, we obtain the set of the singular points of $\tilde{\Xi}_x(z)$:

Lemma B.3 *Let*

$$e^{i\theta_1^{(\pm)}} = \pm\left(\frac{\sin t^{(+)}(\sigma)}{\sqrt{3 - 2\sqrt{2}\cos t^{(+)}(\sigma)}} + \frac{\sqrt{2} - \cos t^{(+)}(\sigma)}{\sqrt{3 - 2\sqrt{2}\cos t^{(+)}(\sigma)}}i\right),$$
$$e^{i\theta_2^{(\pm)}} = \pm\left(\frac{\sin t^{(-)}(\sigma)}{\sqrt{3 - 2\sqrt{2}\cos t^{(-)}(\sigma)}} + \frac{\sqrt{2} - \cos t^{(-)}(\sigma)}{\sqrt{3 - 2\sqrt{2}\cos t^{(-)}(\sigma)}}i\right),$$

where $t^{(\pm)}(\sigma) = \varphi^{(\pm)}(\sigma) - \sigma$ *with*

$$\begin{cases} \cos\varphi^{(\pm)}(\sigma) = \dfrac{1}{\sqrt{2}}\cos\sigma, \\ \sin\varphi^{(\pm)}(\sigma) = \pm\sqrt{1 - \dfrac{1}{2}\cos^2\sigma} \end{cases}.$$

Then, we have the set of all the singular points of $\tilde{\Xi}_x(z)$ *with* $|z| = 1$ *by*

$$B = \begin{cases} B_1 = \{e^{i\theta_1^{(+)}}, e^{i\theta_1^{(-)}}\} & \text{if } \cos\mathrm{t}^{(+)}(\sigma) \le 1/\sqrt{2}, \\ B_2 = \{e^{i\theta_1^{(+)}}, e^{i\theta_1^{(-)}}, e^{i\theta_2^{(+)}}, e^{i\theta_2^{(-)}}\} & \text{if } \cos\mathrm{t}^{(\pm)}(\sigma) \le 1/\sqrt{2}, \\ B_3 = \{e^{i\theta_2^{(+)}}, e^{i\theta_2^{(-)}}\} & \text{if } \cos\mathrm{t}^{(-)}(\sigma) \le 1/\sqrt{2}. \end{cases}$$

The derivation of Lemma B.3 is similar to that of Lemma 4 in Ref. [13]. Here, we omit it.
Next, we derive the residues of $\tilde{\Xi}_x(z)$ at the singular points. For the simplicity, we put the denominator of $\tilde{\Xi}_0(z)$ by $\tilde{\Lambda}_0(z) \equiv 1 - e^{-i\sigma_+}\tilde{f}_0^{(+)}(z)/\sqrt{2} - e^{i\sigma_+}\tilde{f}_0^{(-)}(z)/\sqrt{2} + \tilde{f}_0^{(+)}(z)\tilde{f}_0^{(-)}(z)$. Note that all the singular points for localization come from the solution of

$$\tilde{\Lambda}_0(z) = 0.$$

Then, explicit expressions of the square of the absolute value of the residues of $1/\tilde{\Lambda}_0(z)$ are given in a similar way as that of Lemma 5 in Ref. [13], and we obtain Lemma B.4:

Lemma B.4 *1. For $e^{i\theta_1^{(\pm)}}$, we have*

$$\left|Res\left(\frac{1}{\tilde{\Lambda}_0(z)} : z = e^{i\theta_1^{(\pm)}}\right)\right|^2 = \frac{\left(1-\sqrt{2}\cos t^{(+)}(\sigma)\right)^2}{\left(3-2\sqrt{2}\cos t^{(+)}(\sigma)\right)^2\left\{5+\cos 2\sigma - 2\sqrt{2}\cos(2\sigma + t^{(+)}(\sigma)) - 2\sqrt{2}\cos t^{(+)}(\sigma)\right\}}. \tag{B.3}$$

2. For $e^{i\theta_2^{(\pm)}}$, we have

$$\left|Res\left(\frac{1}{\tilde{\Lambda}_0(z)} : z = e^{i\theta_2^{(\pm)}}\right)\right|^2 = \frac{\left(1-\sqrt{2}\cos t^{(-)}(\sigma)\right)^2}{\left(3-2\sqrt{2}\cos t^{(-)}(\sigma)\right)^2\left\{5+\cos 2\sigma - 2\sqrt{2}\cos(2\sigma + t^{(-)}(\sigma)) - 2\sqrt{2}\cos t^{(-)}(\sigma)\right\}}. \tag{B.4}$$

Noting Lemma B.1-B.4, we first show the case of $x = 0$ in Theorem 2 in the following way. By Lemma B.1, we have

$$\tilde{\Xi}_0(z)\varphi_0 = \frac{1}{\tilde{\Lambda}_0(z)}\begin{bmatrix} \alpha\left(1-\frac{e^{i\sigma_+}}{\sqrt{2}}\tilde{f}_0^{(-)}(z)\right) - \frac{\beta}{\sqrt{2}}\tilde{f}_0^{(+)}(z) \\ \frac{\alpha}{\sqrt{2}}\tilde{f}_0^{(-)}(z) + \beta\left(1-\frac{e^{-i\sigma_+}}{\sqrt{2}}\tilde{f}_0^{(+)}(z)\right)\end{bmatrix}.$$

Thus, we get the square norm of the residues by

$$\left\|Res(\tilde{\Xi}_0(z)\varphi_0 : z = e^{i\theta_j^{(\pm)}})\right\|_{j=1,2}^2 = \left|Res\left(\frac{\alpha\left(1-e^{i\sigma_+}\tilde{f}_0^{(-)}(z)/\sqrt{2}\right) - \beta\tilde{f}_0^{(+)}(z)/\sqrt{2}}{\tilde{\Lambda}_0(z)} : z = e^{i\theta_j^{(\pm)}}\right)\right|^2 + \left|Res\left(\frac{\alpha\tilde{f}_0^{(-)}(z)/\sqrt{2} + \beta\left(1-e^{-i\sigma_+}\tilde{f}_0^{(+)}(z)/\sqrt{2}\right)}{\tilde{\Lambda}_0(z)} : z = e^{i\theta_j^{(\pm)}}\right)\right|^2. \tag{B.5}$$

Taking into account that

$$Res(1/\tilde{\Lambda}_0(z) : z = e^{i\theta_j^{(\pm)}}) = \lim_{z\to e^{i\theta_j^{(\pm)}}}(z - e^{i\theta_j^{(\pm)}})/\tilde{\Lambda}_0(z) \quad (j = 1, 2)$$

holds, where $\{e^{i\theta_j^{(\pm)}}\}_{j=1,2}$ is the set of the singular points of $\tilde{\Xi}_x(z)$, we obtain

$$\left|Res\left(\frac{1}{\tilde{\Lambda}_0(z)} : z = e^{i\theta_j^{(\pm)}}\right)\right|_{j=1,2}^2 = \frac{1}{\left|\tilde{\Lambda}_0'(e^{i\theta_j^{(\pm)}})\right|^2} = \frac{2}{\left|1+\frac{\partial\tilde{\phi}(\theta)}{\partial\theta}\right|_{\theta_j^{(\pm)}}^2\left|1+e^{2i\sigma}-2\sqrt{2}e^{i(2\sigma+\theta_j^{(\pm)}+\tilde{\phi}(\theta_j^{(\pm)}))}\right|^2}, \tag{B.6}$$

with

$$\tilde{\Lambda}_0'(z) = \frac{\partial \tilde{\Lambda}_0(z)}{\partial z}.$$

Thereby, we see from Eq. (B.6),

$$\left| Res\left(\frac{\alpha\left(1 - e^{i\sigma_+}\tilde{f}_0^{(-)}(z)/\sqrt{2}\right) - \beta \tilde{f}_0^{(+)}(z)/\sqrt{2}}{\tilde{\Lambda}_0(z)} : z = e^{i\theta_j^{(\pm)}} \right) \right|_{j=1,2}^2$$
$$= \frac{2\left|\alpha\left(1 - e^{i\sigma_+}\tilde{f}_0^{(-)}(e^{i\theta_j^{(\pm)}})/\sqrt{2}\right) - \beta \tilde{f}_0^{(+)}(e^{i\theta_j^{(\pm)}})/\sqrt{2}\right|^2}{\left|1 + \frac{\partial \tilde{\phi}(\theta)}{\partial \theta}\right|_{\theta_j^{(\pm)}}^2 \left|1 + e^{2i\sigma} - 2\sqrt{2}e^{i(2\sigma + \theta_j^{(\pm)} + \tilde{\phi}(\theta_j^{(\pm)}))}\right|^2},$$

$$\left| Res\left(\frac{\alpha \tilde{f}_0^{(-)}(z)/\sqrt{2} + \beta\left(1 - e^{-i\sigma_+}\tilde{f}_0^{(+)}(z)/\sqrt{2}\right)}{\tilde{\Lambda}_0(z)} : z = e^{i\theta_j^{(\pm)}} \right) \right|_{j=1,2}^2$$
$$= \frac{2\left|\alpha \tilde{f}_0^{(-)}(e^{i\theta_j^{(\pm)}})/\sqrt{2} + \beta\left(1 - e^{-i\sigma_+}\tilde{f}_0^{(+)}(e^{i\theta_j^{(\pm)}})/\sqrt{2}\right)\right|^2}{\left|1 + \frac{\partial \tilde{\phi}(\theta)}{\partial \theta}\right|_{\theta_j^{(\pm)}}^2 \left|1 + e^{2i\sigma} - 2\sqrt{2}e^{i(2\sigma + \theta_j^{(\pm)} + \tilde{\phi}(\theta_j^{(\pm)}))}\right|^2}.$$

Here, we have

$$\left|\alpha\left(1 - \frac{e^{i\sigma_+}\tilde{f}_0^{(-)}(e^{i\theta_j^{(\pm)}})}{\sqrt{2}}\right) - \frac{\beta \tilde{f}_0^{(+)}(e^{i\theta_j^{(\pm)}})}{\sqrt{2}}\right|^2$$
$$= \left\{ a^2\left(\frac{3}{2} - \sqrt{2}\cos(2\sigma + \theta_j^{(\pm)} + \tilde{\phi}(\theta_j^{(\pm)}))\right) + \frac{b^2}{2} - \sqrt{2}ab\cos(\tilde{\phi}_{12} - \theta_j^{(\pm)} - \sigma_+ - \tilde{\phi}(\theta_j^{(\pm)})) + ab\cos(\tilde{\phi}_{12} - \sigma_-)\right\},$$

$$\left|\frac{\alpha \tilde{f}_0^{(-)}(e^{i\theta_j^{(\pm)}})}{\sqrt{2}} + \beta\left(1 - \frac{e^{-i\sigma_+}\tilde{f}_0^{(+)}(e^{i\theta_j^{(\pm)}})}{\sqrt{2}}\right)\right|^2$$
$$= \left\{ \frac{a^2}{2} + b^2\left(\frac{3}{2} - \sqrt{2}\cos(\theta_j^{(\pm)} + \tilde{\phi}(\theta_j^{(\pm)}))\right) + \sqrt{2}ab\cos(\tilde{\phi}_{12} + \theta_j^{(\pm)} - \sigma_- + \tilde{\phi}(\theta_j^{(\pm)})) - ab\cos(\tilde{\phi}_{12} - \sigma_-)\right\}.$$

Therefore, we get

$$\left\| Res(\tilde{\Xi}_0(z)\varphi_0 : z = e^{i\theta_j^{(\pm)}}) \right\|_{j=1,2}^2 = \frac{2}{\left|1 + \frac{\partial \tilde{\phi}(\theta)}{\partial \theta}\right|_{\theta_j^{(\pm)}}^2 \left|1 + e^{2i\sigma} - 2\sqrt{2}e^{i(2\sigma + \theta_j^{(\pm)} + \tilde{\phi}(\theta_j^{(\pm)}))}\right|^2}$$
$$\times \left\{ 2 - \sqrt{2}(a^2\cos(2\sigma + \theta_j^{(\pm)} + \tilde{\phi}(\theta_j^{(\pm)})) + b^2\cos(\theta_j^{(\pm)} + \tilde{\phi}(\theta_j^{(\pm)}))) - \sqrt{2}ab(\cos(\tilde{\phi}_{12} - \sigma_+ - \theta_j^{(\pm)} - \tilde{\phi}(\theta_j^{(\pm)})) \right.$$
$$\left. - \cos(\tilde{\phi}_{12} - \sigma_- + \theta_j^{(\pm)} + \tilde{\phi}(\theta_j^{(\pm)}))) \right\}.$$

Noting

$$\overline{\mu}_{\infty}(0) = \sum_{\theta_j^{(\pm)}} \left\| Res(\tilde{\Xi}_0(z)\varphi_0 : z = e^{i\theta_j^{(\pm)}}) \right\|^2, \tag{B.7}$$

we obtain the case of $x = 0$ in Theorem 2.
Here, the range of the summation is

$$\{\theta_j^{(\pm)} \in [0, 2\pi); e^{i\theta_j^{(\pm)}} \in B\}.$$

In the next stage, we give the detail of the derivation for the case of $x \geq 1$ in Theorem 2. By Lemma B.1, we see

$$\tilde{\Xi}_x(z)\varphi_0 = \frac{(\tilde{\lambda}^{(+)}(z))^{x-1}}{\sqrt{2}\tilde{\Lambda}_0(z)} \begin{bmatrix} (\tilde{\lambda}^{(+)}(z)) \left\{ \alpha e^{i(\theta+\tilde{\phi}(\theta))} - \sqrt{2}\alpha \tilde{f}_0^{(+)}(z)\tilde{f}_0^{(-)}(z) - \beta \tilde{f}_0^{(+)}(z) \right\} \\ z \left\{ \alpha e^{-i\sigma_+} - \sqrt{2}\alpha \tilde{f}_0^{(-)}(z) - \beta \right\} \end{bmatrix} \qquad (x \geq 1).$$

Thereby, we get the square norm of the residues as

$$\begin{aligned} \left\| Res(\tilde{\Xi}_x(z)\varphi_0 : z = e^{i\theta_j^{(\pm)}}) \right\|^2 &= \left| Res \left(\frac{(\tilde{\lambda}^{(+)}(z))^x \left\{ \alpha e^{i(\theta+\tilde{\phi}(\theta))} - \sqrt{2}\alpha \tilde{f}_0^{(+)}(z)\tilde{f}_0^{(-)}(z) - \beta \tilde{f}_0^{(+)}(z) \right\}}{\sqrt{2}\tilde{\Lambda}_0(z)} : z = e^{i\theta_j^{(\pm)}} \right) \right|^2 \\ &+ \left| Res \left(\frac{(\tilde{\lambda}^{(+)}(z))^{x-1} z \left\{ \alpha e^{-i\sigma_+} - \sqrt{2}\alpha \tilde{f}_0^{(-)}(z) - \beta \right\}}{\sqrt{2}\tilde{\Lambda}_0(z)} : z = e^{i\theta_j^{(\pm)}} \right) \right|^2. \end{aligned} \tag{B.8}$$

Taking account of

$$\begin{aligned} &Res \left(\frac{(\tilde{\lambda}^{(+)}(z))^x \left\{ \alpha e^{i(\theta+\tilde{\phi}(\theta))} - \sqrt{2}\alpha \tilde{f}_0^{(+)}(z)\tilde{f}_0^{(-)}(z) - \beta \tilde{f}_0^{(+)}(z) \right\}}{\sqrt{2}\tilde{\Lambda}_0(z)} : z = e^{i\theta_j^{(\pm)}} \right) \\ &= \frac{\left(\tilde{\lambda}^{(+)}(e^{i\theta_j^{(\pm)}}) \right)^x \left(\alpha e^{i(\theta_j^{(\pm)}+\tilde{\phi}(\theta_j^{(\pm)}))} - \sqrt{2}\alpha \tilde{f}_0^{(+)}(e^{i\theta_j^{(\pm)}})\tilde{f}_0^{(-)}(e^{i\theta_j^{(\pm)}}) - \beta \tilde{f}_0^{(+)}(e^{i\theta_j^{(\pm)}}) \right)}{\sqrt{2}\tilde{\Lambda}_0'(e^{i\theta_j^{(\pm)}})}, \end{aligned}$$

we get

$$\begin{aligned} &\left| Res \left(\frac{(\tilde{\lambda}^{(+)}(z))^x \left\{ \alpha e^{i(\theta+\tilde{\phi}(\theta))} - \sqrt{2}\alpha \tilde{f}_0^{(+)}(z)\tilde{f}_0^{(-)}(z) - \beta \tilde{f}_0^{(+)}(z) \right\}}{\sqrt{2}\tilde{\Lambda}_0(z)} : z = e^{i\theta_j^{(\pm)}} \right) \right|^2 \\ &= \frac{\left| \tilde{\lambda}^{(+)}(e^{i\theta_j^{(\pm)}}) \right|^{2x} \left| \alpha e^{i(\theta_j^{(\pm)}+\tilde{\phi}(\theta_j^{(\pm)}))} - \sqrt{2}\alpha \tilde{f}_0^{(+)}(e^{i\theta_j^{(\pm)}})\tilde{f}_0^{(-)}(e^{i\theta_j^{(\pm)}}) - \beta \tilde{f}_0^{(+)}(e^{i\theta_j^{(\pm)}}) \right|^2}{\left| 1 + \frac{\partial \tilde{\phi}(\theta)}{\partial \theta} \right|_{\theta_j^{(\pm)}}^2 \left| 1 + e^{2i\sigma} - 2\sqrt{2}e^{i(2\sigma+\theta_j^{(\pm)}+\tilde{\phi}(\theta_j^{(\pm)}))} \right|^2}. \end{aligned} \tag{B.9}$$

In a similar fashion, we obtain

$$\left| Res\left(\frac{(\tilde{\lambda}^{(+)}(z))^{x-1} z \left\{ \alpha e^{-i\sigma_+} - \sqrt{2}\alpha \tilde{f}_0^{(-)}(z) - \beta \right\}}{\sqrt{2}\tilde{\Lambda}_0(z)} : z = e^{i\theta_j^{(\pm)}} \right) \right|^2$$
$$= \frac{\left|\tilde{\lambda}^{(+)}(e^{i\theta_j^{(\pm)}})\right|^{2(x-1)} \left| \alpha e^{-i\sigma_+} - \sqrt{2}\alpha \tilde{f}_0^{(-)}(e^{i\theta_j^{(\pm)}}) - \beta \right|^2}{\left| 1 + \frac{\partial \tilde{\phi}(\theta)}{\partial \theta} \right|_{\theta_j^{(\pm)}}^2 \left| 1 + e^{2i\sigma} - 2\sqrt{2} e^{i(2\sigma + \theta_j^{(\pm)} + \tilde{\phi}(\theta_j^{(\pm)}))} \right|^2}. \quad \text{(B.10)}$$

Thereby, Eqs. (B.8), (B.9) and (B.10) provide

$$\left\| Res(\tilde{\Xi}_x(z)\varphi_0 : z = e^{i\theta_j^{(\pm)}}) \right\|_{j=1,2}^2 = \frac{\left|\tilde{\lambda}^{(+)}(e^{i\theta_j^{(\pm)}})\right|^{2(x-1)}}{\left| 1 + \frac{\partial \tilde{\phi}(\theta)}{\partial \theta} \right|_{\theta_j^{(\pm)}}^2 \left| 1 + e^{2i\sigma} - 2\sqrt{2} e^{i(2\sigma + \theta_j^{(\pm)} + \tilde{\phi}(\theta_j^{(\pm)}))} \right|^2} \left(1 + \left|\tilde{\lambda}^{(+)}(e^{i\theta_j^{(\pm)}})\right|^2 \right)$$
$$\times \left\{ 1 + 2a^2 - 2\sqrt{2}a^2 \cos(2\sigma + \theta_j^{(\pm)} + \tilde{\phi}(\theta_j^{(\pm)})) - 2ab \left(\cos(\tilde{\phi}_{12} - \sigma_+) - \sqrt{2}\cos(\tilde{\phi}_{12} - \sigma_- + \theta_j^{(\pm)} + \tilde{\phi}(\theta_j^{(\pm)})) \right) \right\}.$$

Hence, we obtain

$$\overline{\mu}_\infty(x) = \sum_{\theta_j^{(\pm)}} \frac{\left|\tilde{\lambda}^{(+)}(e^{i\theta_j^{(\pm)}})\right|^{2(x-1)}}{\left| 1 + \frac{\partial \tilde{\phi}(\theta)}{\partial \theta} \right|_{\theta_j^{(\pm)}}^2 \left| 1 + e^{2i\sigma} - 2\sqrt{2} e^{i(2\sigma + \theta_j^{(\pm)} + \tilde{\phi}(\theta_j^{(\pm)}))} \right|^2} \left(1 + \left|\tilde{\lambda}^{(+)}(e^{i\theta_j^{(\pm)}})\right|^2 \right)$$
$$\times \left\{ 1 + 2a^2 - 2\sqrt{2}a^2 \cos(2\sigma + \theta_j^{(\pm)} + \tilde{\phi}(\theta_j^{(\pm)})) - 2ab \left(\cos(\tilde{\phi}_{12} - \sigma_+) - \sqrt{2}\cos(\tilde{\phi}_{12} - \sigma_- + \theta_j^{(\pm)} + \tilde{\phi}(\theta_j^{(\pm)})) \right) \right\}, \quad \text{(B.11)}$$

where $\{e^{i\theta_j^{(\pm)}}\}_{j=1,2}$ is the set of the singular points of $\tilde{\Xi}_x(z)$. Now, we compute $\left|\tilde{\lambda}^{(+)}(e^{i\theta_j^{(\pm)}})\right|^2$. By the definition of $\tilde{\lambda}^{(+)}(z)$ in Lemma B.1, we see

$$\tilde{\lambda}^{(+)}(e^{i\theta}) = \frac{1}{e^{i\tilde{\phi}(\theta)} - \sqrt{2}e^{-i\theta}}$$

which leads to

$$\left|\tilde{\lambda}^{(+)}(e^{i\theta})\right|^2 = \frac{1}{3 - 2\sqrt{2}\cos(\theta + \tilde{\phi}(\theta))},$$

Equation (B.2) gives

$$\begin{cases} \left|\tilde{\lambda}^{(+)}(e^{i\theta_1^{(\pm)}})\right|^2 = \dfrac{1}{3 - 2\sqrt{2}\cos t^{(+)}(\sigma)}, \\ \left|\tilde{\lambda}^{(+)}(e^{i\theta_2^{(\pm)}})\right|^2 = \dfrac{1}{3 + 2\sqrt{2}\cos t^{(-)}(\sigma)}. \end{cases} \quad \text{(B.12)}$$

Taking into account Proposition 2, and substituting Lemma B.4 and Eq. (B.12) into Eq. (B.11), we obtain the case of $x \geq 1$ in Theorem 2. In a similar fashion, we get the case of $x \leq -1$ in Theorem 2, and we complete the proof.

Appendix C

In Appendix C, we give the proof of Theorem 3 in a similar way as Appendix A in Ref. [17]. Now, we consider the characteristic function of QW:

$$E\left[e^{i\xi\frac{X_t}{t}}\right] = \int_{x\in\mathbb{Z}} g_{X_t/t}(x)e^{i\xi x}dx, \tag{C.1}$$

where $g_{X_t/t}(x)$ is the density function of random variable X_t/t. Hereafter, we rewrite $E\left[e^{iX_t/t}\right]$ $(t\to\infty)$ to obtain the explicit expression of $w(x)f_K(x;1/\sqrt{2})$. By a simple argument, we obtain

Proposition 3

$$E\left[e^{i\xi\frac{X_t}{t}}\right] \to \int_0^{2\pi}\sum_{\theta\in A} e^{-i\xi\theta^{'}(k)}\left\|Res(\hat{\tilde{\Xi}}(k:z):z=e^{i\theta(k)})\right\|^2\frac{dk}{2\pi} \qquad (t\to\infty), \tag{C.2}$$

where A is the set of the singular points of $\hat{\tilde{\Xi}}(k:z)\equiv\sum_{x\in\mathbb{Z}}\tilde{\Xi}_x(z)e^{ikx}$ with $\tilde{\Xi}_x(z)=\sum_t\Xi_t(x)z^t$. Note $\theta^{'}(k)=\partial\theta(k)/\partial k$.

The proof of Proposition 3 is given in Ref. [14]. By mainly using Proposition 3, we prove Theorem 3.
First of all, we derive the singular points of $\hat{\tilde{\Xi}}(k:z)$ and then, compute the residues of $\hat{\tilde{\Xi}}(k:z)$ at the singular points. By Lemma B.1, we can rewrite $\hat{\tilde{\Xi}}(k:z)$ as

$$\begin{aligned}\hat{\tilde{\Xi}}(k:z) = \Bigg\{ &\frac{e^{ik}}{1-e^{ik}\tilde{\lambda}^{(+)}(z)}\begin{bmatrix}\tilde{\lambda}^{(+)}(z)\tilde{f}_0^{(+)}(z)\\ z\end{bmatrix}\begin{bmatrix}\frac{e^{-i\sigma_+}}{\sqrt{2}}, -\frac{1}{\sqrt{2}}\end{bmatrix}\\ &+\frac{e^{-ik}}{1-e^{-ik}\tilde{\lambda}^{(-)}(z)}\begin{bmatrix}z\\ \tilde{\lambda}^{(-)}(z)\tilde{f}_0^{(-)}(z)\end{bmatrix}\begin{bmatrix}\frac{1}{\sqrt{2}}, \frac{e^{i\sigma_+}}{\sqrt{2}}\end{bmatrix} + I\Bigg\}\tilde{\Xi}_0(z).\end{aligned} \tag{C.3}$$

Note that if $|z|<1$, then $|\tilde{\lambda}^{(\pm)}(z)|<1$ holds, and the infinite series $\sum_x(\tilde{\lambda}^{(+)}(z))^{|x|-1}e^{ikx}$ and $\sum_x(\tilde{\lambda}^{(-)}(z))^{|x|-1}e^{-ikx}$ converge. According to Ref. [31], we have

$$\begin{cases}\tilde{\lambda}^{(\pm)}(e^{i\theta}) = \mp\{\mathrm{sgn}(\cos\theta)\sqrt{2\cos^2\theta-1}+i\sqrt{2}\sin\theta\}\\ \tilde{f}_0^{(\pm)}(e^{i\theta}) = \mathrm{sgn}(\cos\theta)e^{i(\theta\pm\sigma_\pm)}\{\sqrt{2}|\cos\theta|-\sqrt{2\cos^2\theta-1}\}\end{cases}, \tag{C.4}$$

which can be derived in a similar way as relation (4.25) in Ref. [17]. The singular points derived from $\tilde{\Xi}_0(z)$ are related with localization, while principal singular points for weak convergence come from

$$1-e^{ik}\tilde{\lambda}^{(+)}(z)=0, \tag{C.5}$$

and

$$1-e^{-ik}\tilde{\lambda}^{(-)}(z)=0. \tag{C.6}$$

For Eq. (C.5), we see

$$\cos k = -\,\mathrm{sgn}(\cos\theta^{(+)}(k))\sqrt{2\cos^2\theta^{(+)}(k)-1}, \tag{C.7}$$

$$\sin k = \sqrt{2}\sin\theta^{(+)}(k), \tag{C.8}$$

and for Eq. (C.6), we have

$$\cos k = \mathrm{sgn}(\cos\theta^{(-)}(k)(k))\sqrt{2\cos^2\theta^{(-)}(k) - 1}, \tag{C.9}$$

$$\sin k = \sqrt{2}\sin\theta^{(-)}(k). \tag{C.10}$$

Put $-\partial\theta^{(\pm)}(k)/\partial k = x_\pm$ to compute the RHS of Eq. (C.2). Derivating Eqs. (C.7) and (C.9) with respect to k, we obtain $\sin k$, $\cos k$, $\sin\theta^{(\pm)}(k)$, and $\cos\theta^{(\pm)}(k)$ as follows: Equations (C.7) and (C.8) give

$$\begin{cases} \cos k = \mathrm{sgn}(\cos k)\dfrac{x_+}{\sqrt{1-x_+^2}},\ \cos\theta^{(+)}(k) = -\,\mathrm{sgn}(\cos k)\dfrac{1}{\sqrt{2(1-x_+^2)}}, \\ \sin k = \mathrm{sgn}(\sin k)\sqrt{\dfrac{1-2x_+^2}{1-x_+^2}},\ \ \sin\theta^{(+)}(k) = \mathrm{sgn}(\sin k)\sqrt{\dfrac{1-2x_+^2}{2(1-x_+^2)}}. \end{cases} \tag{C.11}$$

Equations (C.9) and (C.10) provide

$$\begin{cases} \cos k = \mathrm{sgn}(\cos k)\dfrac{x_-}{\sqrt{1-x_-^2}},\ \cos\theta^{(-)}(k) = \mathrm{sgn}(\cos k)\dfrac{1}{\sqrt{2(1-x_-^2)}}, \\ \sin k = \mathrm{sgn}(\sin k)\sqrt{\dfrac{1-2x_-^2}{1-x_-^2}},\ \ \sin\theta^{(-)}(k) = \mathrm{sgn}(\sin k)\sqrt{\dfrac{1-2x_-^2}{2(1-x_-^2)}}. \end{cases} \tag{C.12}$$

Thereby, we obtain A, the set of the singular points of $\hat{\tilde{\Xi}}(k:z)$:

$$A = \{e^{i\theta^{(+)}(k)}, e^{i\theta^{(-)}(k)}\},$$

with

$$e^{i\theta^{(+)}(k)} = -\frac{\mathrm{sgn}(\cos k)}{\sqrt{2(1-x_+^2)}} + i\,\mathrm{sgn}(\sin k)\sqrt{\frac{1-2x_+^2}{2(1-x_+^2)}},$$

and

$$e^{i\theta^{(-)}(k)} = \frac{\mathrm{sgn}(\cos k)}{\sqrt{2(1-x_-^2)}} + i\,\mathrm{sgn}(\sin k)\sqrt{\frac{1-2x_-^2}{2(1-x_-^2)}}.$$

Next, we compute the residue of $\hat{\tilde{\Xi}}(k;z)$ at $e^{i\theta^{(\pm)}(k)}$. Substituting the singular points to $\tilde{f}_0^{(\pm)}(z)$, we get

1. $\tilde{f}_0^{(+)}(e^{i\theta^{(+)}(k)}) = -\,\mathrm{sgn}(\cos k)e^{i(\theta^+(k)+\sigma_+)}\dfrac{\sqrt{1-x_\pm^2}}{1+|x_\pm|}$,
   $\tilde{f}_0^{(-)}(e^{i\theta^{(+)}(k)}) = -\,\mathrm{sgn}(\cos k)e^{i(\theta^{(+)}(k)-\sigma_-)}\dfrac{\sqrt{1-x_\pm^2}}{1+|x_\pm|}$,

2. $\tilde{f}_0^{(+)}(e^{i\theta^{(-)}(k)}) = \mathrm{sgn}(\cos k) e^{i(\theta^{(-)}(k)+\sigma_+)} \dfrac{\sqrt{1-x_\pm^2}}{1+|x_\pm|}$,

$\tilde{f}_0^{(-)}(e^{i\theta^{(-)}(k)}) = \mathrm{sgn}(\cos k) e^{i(\theta^{(-)}(k)-\sigma_-)} \dfrac{\sqrt{1-x_\pm^2}}{1+|x_\pm|}$.

Taking into account Lemma B.1, we have

$$\begin{aligned}
&\frac{e^{ik}}{1-e^{ik}\tilde{\lambda}^{(+)}(z)} \begin{bmatrix} \tilde{f}_0^{(+)}(z)\tilde{\lambda}^{(+)}(z) \\ z \end{bmatrix} \left[\frac{e^{-i\sigma_+}}{\sqrt{2}}, -\frac{1}{\sqrt{2}} \right] \tilde{\Xi}_0(z) \\
&\qquad = \frac{1}{\tilde{\Lambda}_0(z)} \frac{e^{ik}}{1-e^{ik}\tilde{\lambda}^{(+)}(z)} \begin{bmatrix} \tilde{f}_0^{(+)}(z)\tilde{\lambda}^{(+)}(z) \\ z \end{bmatrix} \frac{1}{\sqrt{2}} \left\{ \alpha \left(e^{-i\sigma_+} - \sqrt{2}\tilde{f}_0^{(-)}(z) \right) - \beta \right\},
\end{aligned}$$

and the square norm of residue of the first term of Eq. (C.3) is written by

$$\begin{aligned}
&\left| Res \left(\frac{e^{ik}}{1-e^{ik}\tilde{\lambda}^{(+)}(z)} \begin{bmatrix} \tilde{f}_0^{(+)}(z)\tilde{\lambda}^{(+)}(z) \\ z \end{bmatrix} \left[\frac{e^{-i\sigma_+}}{\sqrt{2}}, -\frac{1}{\sqrt{2}} \right] \tilde{\Xi}_0(z) : z = e^{i\theta^{(+)}(k)} \right) \right|^2 \\
&\qquad = \left| Res \left(\frac{1}{1-e^{ik}\tilde{\lambda}^{(+)}(z)} : z = e^{i\theta^{(+)}(k)} \right) \right|^2 \left\| \begin{bmatrix} \tilde{f}_0^{(+)}(e^{i\theta^{(+)}(k)})\tilde{\lambda}^{(+)}(e^{i\theta^{(+)}(k)}) \\ e^{i\theta^{(+)}(k)} \end{bmatrix} \right\|^2 \\
&\qquad\qquad \times \frac{1}{2\left|\tilde{\Lambda}_0(e^{i\theta^{(+)}(k)})\right|^2} \left| \alpha \left(e^{-i\sigma_+} - \sqrt{2}\tilde{f}_0^{(-)}(e^{i\theta^{(+)}(k)}) \right) - \beta \right|^2.
\end{aligned}$$

In a similar fashion, the square norm of residue of the second term of Eq. (C.3) becomes

$$\begin{aligned}
&\left| Res \left(\frac{e^{-ik}}{1-e^{-ik}\tilde{\lambda}^{(-)}(z)} \begin{bmatrix} z \\ \tilde{f}_0^{(-)}(z)\tilde{\lambda}^{(-)}(z) \end{bmatrix} \left[\frac{1}{\sqrt{2}}, \frac{e^{i\sigma_+}}{\sqrt{2}} \right] \tilde{\Xi}_0(z) : z = e^{i\theta^{(-)}(k)} \right) \right|^2 \\
&\qquad = \left| Res \left(\frac{1}{1-e^{-ik}\tilde{\lambda}^{(-)}(z)} : z = e^{i\theta^{(-)}(k)} \right) \right|^2 \left\| \begin{bmatrix} e^{i\theta^{(-)}(k)} \\ \tilde{f}_0^{(-)}(e^{i\theta^{(-)}(k)})\tilde{\lambda}^{(-)}(e^{i\theta^{(-)}(k)}) \end{bmatrix} \right\|^2 \\
&\qquad\qquad \times \frac{1}{2\left|\tilde{\Lambda}_0(e^{i\theta^{(-)}(k)})\right|^2} \left| \alpha + \beta \left(e^{i\sigma_+} - \sqrt{2}\tilde{f}^{(+)}(e^{i\theta^{(-)}(k)}) \right) \right|^2.
\end{aligned}$$

Thereby, we obtain

$$\begin{aligned}
\left\| Res(\hat{\tilde{\Xi}}(k:z) : z = e^{i\theta^{(\pm)}(k)}) \right\|^2 &= \left| Res \left(\frac{1}{1-e^{ik}\tilde{\lambda}^{(+)}(z)} : z = e^{i\theta^{(+)}(k)} \right) \right|^2 \left\| \begin{bmatrix} \tilde{f}_0^{(+)}(e^{i\theta^{(+)}(k)})\tilde{\lambda}^{(+)}(e^{i\theta^{(+)}(k)}) \\ e^{i\theta^{(+)}(k)} \end{bmatrix} \right\|^2 \\
&\qquad \times \frac{1}{2\left|\tilde{\Lambda}_0(e^{i\theta^{(+)}(k)})\right|^2} \left| \alpha \left(e^{-i\sigma_+} - \sqrt{2}\tilde{f}_0^{(-)}(e^{i\theta^{(+)}(k)}) \right) - \beta \right|^2 \\
&\quad + \left| Res \left(\frac{1}{1-e^{-ik}\tilde{\lambda}^{(-)}(z)} : z = e^{i\theta^{(-)}(k)} \right) \right|^2 \left\| \begin{bmatrix} e^{i\theta^{(-)}(k)} \\ \tilde{f}_0^{(-)}(e^{i\theta^{(-)}(k)})\tilde{\lambda}^{(-)}(e^{i\theta^{(-)}(k)}) \end{bmatrix} \right\|^2 \\
&\qquad \times \frac{1}{2\left|\tilde{\Lambda}_0(e^{i\theta^{(-)}(k)})\right|^2} \left| \alpha + \beta \left(e^{i\sigma_+} - \sqrt{2}\tilde{f}^{(+)}(e^{i\theta^{(-)}(k)}) \right) \right|^2 . \quad \text{(C.13)}
\end{aligned}$$

Hereafter, we will write the items below with respect to x_+ or x_-, and then substitute those in Eq. (C.13).

- $\left|Res\left(\frac{1}{1-e^{ik}\tilde{\lambda}^{(+)}(z)} : z = e^{i\theta^{(+)}(k)}\right)\right|^2$ and $\left|Res\left(\frac{1}{1-e^{-ik}\tilde{\lambda}^{(-)}(z)} : z = e^{i\theta^{(-)}(k)}\right)\right|^2$.
- $\frac{1}{\left|\tilde{\Lambda}_0(e^{i\theta^{(\pm)}(k)})\right|^2}$.
- $\frac{1}{2}\left|\alpha\left(e^{-i\sigma_+} - \sqrt{2}\tilde{f}_0^{(-)}(e^{i\theta^{(+)}(k)})\right) - \beta\right|^2$ and $\frac{1}{2}\left|\alpha + \beta\left(e^{i\sigma_+} - \sqrt{2}\tilde{f}^{(+)}(e^{i\theta^{(-)}(k)})\right)\right|^2$.
- $\left\|\begin{bmatrix}\tilde{\lambda}^{(+)}(e^{i\theta^{(+)}(k)})\tilde{f}_0^{(+)}(e^{i\theta^{(+)}(k)}) \\ e^{i\theta^{(+)}(k)}\end{bmatrix}\right\|^2$ and $\left\|\begin{bmatrix}e^{i\theta^{(-)}(k)} \\ \tilde{\lambda}^{(-)}(e^{i\theta^{(-)}(k)})\tilde{f}_0^{(-)}(e^{i\theta^{(-)}(k)})\end{bmatrix}\right\|^2$.

(I) Derivation of $\left|Res\left(\frac{1}{1-e^{ik}\tilde{\lambda}^{(+)}(z)} : z = e^{i\theta^{(+)}(k)}\right)\right|^2$ and $\left|Res\left(\frac{1}{1-e^{-ik}\tilde{\lambda}^{(-)}(z)} : z = e^{i\theta^{(-)}(k)}\right)\right|^2$:

Putting $g^{(\pm)}(z) = 1 - e^{\pm ik}\tilde{\lambda}^{(\pm)}(z)$, and we have

$$Res\left(\frac{1}{1-e^{\pm ik}\tilde{\lambda}^{(\pm)}(z)} : z = e^{i\theta^{(\pm)}(k)}\right) = \left.\frac{1}{\frac{\partial g^{(\pm)}(z)}{\partial z}}\right|_{z=e^{i\theta^{(\pm)}(k)}}.$$

Owing to Eq. (C.4), we see

$$\left.\frac{\partial g^{(\pm)}(z)}{\partial z}\right|_{z=e^{i\theta^{(\pm)}(k)}} = \mp i\frac{\mathrm{sgn}(\cos k)}{\sqrt{1-x_\pm^2}}e^{-i(\theta^{(\pm)}(k)\mp k)}\left\{\mathrm{sgn}(\cos k\sin k)\frac{\sqrt{1-2x_\pm^2}}{x_\pm} + i\right\},$$

which lead to

$$\begin{cases}\left|Res\left(\frac{1}{1-e^{ik}\tilde{\lambda}^{(+)}(z)} : z = e^{i\theta^{(\pm)}(k)}\right)\right|^2 = x_+^2, \\ \left|Res\left(\frac{1}{1-e^{-ik}\tilde{\lambda}^{(-)}(z)} : z = e^{i\theta^{(\pm)}(k)}\right)\right|^2 = x_-^2.\end{cases} \tag{C.14}$$

(II) Derivation of $1/\left|\tilde{\Lambda}_0(e^{i\theta^{(\pm)}(k)})\right|^2$: Taking into account Lemma B.1, we have

$$\begin{aligned}\left|\tilde{\Lambda}_0(e^{i\theta})\right|^2 = 1 &+ \left|\tilde{f}_0^{(+)}(e^{i\theta})\right|^2 + \left|\tilde{f}_0^{(+)}(e^{i\theta})\right|^2\left|\tilde{f}_0^{(-)}(e^{i\theta})\right|^2 - \sqrt{2}\Re\left\{e^{-i\sigma_+}\tilde{f}_0^{(+)}(e^{i\theta})\right\} - \sqrt{2}\Re\left\{e^{i\sigma_+}\tilde{f}_0^{(-)}(e^{i\theta})\right\} \\ &+ 2\Re\left\{\tilde{f}_0^{(+)}(e^{i\theta})\tilde{f}_0^{(-)}(e^{i\theta})\right\} + \Re\{e^{-2i\sigma_+}\tilde{f}_0^{(+)}(e^{i\theta})\overline{\tilde{f}_0^{(-)}(e^{i\theta})}\} - \sqrt{2}\Re\left\{e^{-i\sigma_+}\left|\tilde{f}_0^{(+)}(e^{i\theta})\right|^2\overline{\tilde{f}_0^{(-)}(e^{i\theta})}\right\} \\ &- \sqrt{2}\Re\left\{e^{i\sigma_+}\left|\tilde{f}_0^{(-)}(e^{i\theta})\right|^2\overline{\tilde{f}_0^{(+)}(e^{i\theta})}\right\},\end{aligned} \tag{C.15}$$

for $\theta \in \mathbb{R}$. Thereby, substituting the singular points into Eq. (C.15), we obtain

$$\begin{cases} \left|\dfrac{1}{\tilde{\Lambda}_0(e^{i\theta^{(+)}(k)})}\right|^2 = \dfrac{(1+x_+)^2}{2(\sin^2\sigma + x_+^2\cos 2\sigma)}, \\ \left|\dfrac{1}{\tilde{\Lambda}_0(e^{i\theta^{(-)}(k)})}\right|^2 = \dfrac{(1-x_-)^2}{2(\sin^2\sigma + x_-^2\cos 2\sigma)}. \end{cases} \tag{C.16}$$

(Ⅲ) Derivation of $\left|\alpha\left(e^{-i\sigma_+} - \sqrt{2}\tilde{f}_0^{(-)}(e^{i\theta^{(+)}(k)})\right) - \beta\right|^2/2$ and $\left|\alpha + \beta\left(e^{i\sigma_+} - \sqrt{2}\tilde{f}_0^{(+)}(e^{i\theta^{(-)}(k)})\right)\right|^2/2$:

Let the initial coin state be $\varphi_0 = {}^T[\alpha, \beta]$, where $\alpha = ae^{i\phi_1}$, $\beta = be^{i\phi_2}$ with $a, b \in \mathbb{R}$, $a^2 + b^2 = 1$, and $\phi_j \in \mathbb{R}$ $(j = 1, 2)$. Taking account of

$$\begin{aligned} \frac{1}{2}\left|\alpha\left(e^{-i\sigma_+} - \sqrt{2}\tilde{f}_0^{(-)}(e^{i\theta^{(+)}(k)})\right) - \beta\right|^2 = \frac{1}{2} + a^2\left|\tilde{f}_0^{(-)}(e^{i\theta^{(+)}(k)})\right|^2 - \sqrt{2}a^2\Re\{e^{i\sigma_+}\tilde{f}_0^{(-)}(e^{i\theta^{(+)}(k)})\} \\ -\Re\left\{abe^{i\tilde{\phi_{12}}}\left(e^{-i\sigma_+} - \sqrt{2}\tilde{f}_0^{(-)}(e^{i\theta^{(+)}(k)})\right)\right\}, \end{aligned}$$

and

$$\begin{aligned} \frac{1}{2}\left|\alpha + \beta\left(e^{i\sigma_+} - \sqrt{2}\tilde{f}^{(+)}(e^{i\theta^{(-)}(k)})\right)\right|^2 = \frac{1}{2} + b^2\left|\tilde{f}^{(+)}(e^{i\theta^{(-)}(k)})\right|^2 - \sqrt{2}b^2\Re\{e^{-i\sigma_+}\tilde{f}^{(+)}(e^{i\theta^{(-)}(k)})\} \\ +\Re\left\{abe^{i\tilde{\phi_{21}}}\left(e^{i\sigma_+} - \sqrt{2}\tilde{f}^{(+)}(e^{i\theta^{(-)}(k)})\right)\right\}, \end{aligned}$$

we have

$$\begin{cases} \dfrac{1}{2}\left|\alpha\left(e^{-i\sigma_+} - \sqrt{2}\tilde{f}_0^{(-)}(e^{i\theta^{(+)}(k)})\right) - \beta\right|^2 = \dfrac{1}{2} + a^2\dfrac{1-x_+}{1+x_+} - ab\cos\gamma_- \\ -\dfrac{a}{1+x_+}\left\{a\left(\cos 2\sigma + \mathrm{sgn}(\sin k\cos k)\sqrt{1-2x_+^2}\sin 2\sigma\right) - b\left(\cos\gamma_+ + \mathrm{sgn}(\sin k\cos k)\sqrt{1-2x_+^2}\sin\gamma_+\right)\right\}, \\ \dfrac{1}{2}\left|\alpha + \beta\left(e^{i\sigma_+} - \sqrt{2}\tilde{f}^{(+)}(e^{i\theta^{(-)}(k)})\right)\right|^2 = \dfrac{1}{2} + b^2\dfrac{x_-}{1-x_-} - \dfrac{ab}{1-x_-}\left\{x_-\cos\gamma_- - \mathrm{sgn}(\sin k\cos k)\sin\gamma_-\sqrt{1-2x_-^2}\right\}, \end{cases} \tag{C.17}$$

where $\gamma_+ = \tilde{\phi}_{12} - \sigma_-$ and $\gamma_- = \tilde{\phi}_{21} + \sigma_+$ with $\tilde{\phi}_{12} = \phi_1 - \phi_2$.

(Ⅳ) Derivation of $\left\|\begin{bmatrix}\tilde{\lambda}^{(+)}(e^{i\theta^{(+)}(k)})\tilde{f}_0^{(+)}(e^{i\theta^{(+)}(k)}) \\ e^{i\theta^{(+)}(k)}\end{bmatrix}\right\|^2$ and $\left\|\begin{bmatrix}e^{i\theta^{(-)}(k)} \\ \tilde{\lambda}^{(-)}(e^{i\theta^{(-)}(k)})\tilde{f}_0^{(-)}(e^{i\theta^{(-)}(k)})\end{bmatrix}\right\|^2$:

By a simple computation, we have

$$\begin{cases} \left\|\begin{bmatrix}\tilde{\lambda}^{(+)}(e^{i\theta^{(+)}(k)})\tilde{f}_0^{(+)}(e^{i\theta^{(+)}(k)}) \\ e^{i\theta^{(+)}(k)}\end{bmatrix}\right\|^2 = \left|\tilde{\lambda}^{(+)}(e^{i\theta^{(+)}(k)})\right|^2\left|\tilde{f}_0^{(+)}(e^{i\theta^{(+)}(k)})\right|^2 + 1 = \dfrac{2}{1+x_+} \quad (x_+ > 0), \\ \left\|\begin{bmatrix}e^{i\theta^{(-)}(k)} \\ \tilde{\lambda}^{(-)}(e^{i\theta^{(-)}(k)})\tilde{f}_0^{(-)}(e^{i\theta^{(-)}(k)})\end{bmatrix}\right\|^2 = 1 + \left|\tilde{\lambda}^{(-)}(e^{i\theta^{(-)}(k)})\right|^2\left|\tilde{f}_0^{(-)}(e^{i\theta^{(-)}(k)})\right|^2 = \dfrac{2}{1-x_-} \quad (x_- < 0). \end{cases} \tag{C.18}$$

Remark

$$-\frac{\partial\theta^{(\pm)}(k)}{\partial k} = x_{\pm}, \tag{C.19}$$

which gives

$$x_+ = \frac{|\cos k|}{\sqrt{1+\cos^2 k}} \quad x_- = -\frac{|\cos k|}{\sqrt{1+\cos^2 k}}. \tag{C.20}$$

Henceforth, we can treat x_+ and x_- as a valuable x:

$$x = \begin{cases} x_+ & (x>0) \\ x_- & (x<0) \end{cases} .$$

Combining Eqs. (C.11) and (C.12) with Eq. (C.20), and noting Eq. (C.19), we see

$$\frac{dx}{dk} = -\operatorname{sgn}(x)\operatorname{sgn}(\sin k\cos k)(1-x^2)\sqrt{1-2x^2},$$

and thereby we obtain

$$dk = \begin{cases} -\operatorname{sgn}(\sin k\cos k) f_K(x;1/\sqrt{2})\pi dx & (x>0) \\ \operatorname{sgn}(\sin k\cos k) f_K(x;1/\sqrt{2})\pi dx & (x<0) \end{cases} . \tag{C.21}$$

Substituting the items given in (I) to (IV) into Eq. (C.13) and combining with Eq. (C.2), we obtain Theorem 3.

Appendix D

In Appendix D, we derive Eqs. (8) - (10).
It is known that the relevant symmetries for topological phases require Hamiltonian H to satisfy the following relations[5, 10, 20, 37]:

$$T\,H\,T^{-1} = +H \quad \text{(Time-reversal symmetry)}, \tag{D.1a}$$

$$P\,(H-E_P)\,P^{-1} = -(H-E_P) \quad \text{(Particle-hole symmetry)}, \tag{D.1b}$$

$$\Gamma\,(H-E_\Gamma)\,\Gamma^{-1} = -(H-E_\Gamma) \quad \text{(Chiral symmetry)}\ . \tag{D.1c}$$

Here, the operators T and P are anti-unitary operators (i.e., they should contain a complex conjugate operator K), while Γ is a unitary one. Therefore,

$$T^2 = \pm 1, \quad P^2 = \pm 1, \quad \Gamma^2 = +1.$$

In Eqs. (D.1b) and (D.1c), we assume that the Hamiltonian H satisfies the eigenvalue equation $(H-E_X)\boldsymbol{v} = E\boldsymbol{v}$, where X stands for P or Γ, with an eigenvector $\boldsymbol{v}$ and $E, E_X \in \mathbb{R}$. If so, Eqs. (D.1b) and (D.1c) guarantee that $(H-E_X)\cdot X\boldsymbol{v} = -E\cdot X\boldsymbol{v}$, where X stands for P or Γ. Thereby, a pair of eigenvalues with opposite signs $\pm E$ around the symmetric point E_X appears. On the contrary, no special energy is needed to define time-reversal symmetry Eq. (D.1a).
The time-independent Hamiltonian H and the time-evolution operator $U^{(s)}$ for a single time-step are related by

$$U^{(s)} = e^{-iHt/\hbar} \tag{D.2}$$

where t and $\hbar$ represent a time interval of the single time-step operation and a reduced Planck constant, respectively. Hereafter, we simply assume $t = \hbar = 1$. Because of Eq. (D.2), quasi-energy $\varepsilon \in \mathbb{R}$, which has 2π periodicity, is introduced from the eigenvalue λ of the time-evolution operator $U^{(s)}$ in Eq. (4):

$$\lambda = e^{-i\varepsilon}. \tag{D.3}$$

When we derive the constraint of the relevant symmetries for topological phases on the time-evolution operator from Eq. (D.1), we replace E, E_P, and E_Γ of the Hamiltonian with ε, ε_P, and ε_Γ, respectively, in order to emphasize 2π periodicity of quasi-energy.
Using Eqs. (D.1) and (D.2) and considering that only symmetric operators T and P contain the complex conjugate operator K, we obtain the relations in Eqs. (8) - (10).

Appendix E

In Appendix E, we clarify the presence or absence of particle-hole symmetry Eq. (9) and chiral symmetry Eq. (10) of the time-evolution operator of the complete two-phase QW.
To begin with, we rewrite the time-evolution operator so that the argument on the symmetries makes easy. For simplicity, we ignore the position dependence of the phase $\sigma_\pm$ and write it as σ_0 in this appendix. (The symmetries in case of the position dependent phases $\sigma_\pm$ are discussed in the main text.) We also prefer to introduce an additional parameter θ into the coin operator for the sake of general arguments of the topological phase. Therefore, we focus on the following coin in this appendix:

$$U_{\sigma_0,\theta} = \begin{bmatrix} \cos(\theta) & e^{i\sigma_0}\sin(\theta) \\ e^{-i\sigma_0}\sin(\theta) & -\cos(\theta) \end{bmatrix}. \tag{E.1}$$

Note that $U_+ = U_{\sigma_+,\pi/4}$ and $U_- = U_{\sigma_-,\pi/4}$.
We also introduce the split-shift operator $S_\pm$ defined as

$$S_+ = \sum_x \left(|x\rangle\langle x| \otimes |L\rangle\langle L| + |x\rangle\langle x-1| \otimes |R\rangle\langle R| \right), \tag{E.2a}$$

$$S_- = \sum_x \left(|x\rangle\langle x+1| \otimes |L\rangle\langle L| + |x\rangle\langle x| \otimes |R\rangle\langle R| \right). \tag{E.2b}$$

Note that multiplying S_+ and S_- gives the standard shift operator: $S = S_+S_- = S_-S_+$.
In order to study the relevant symmetries for topological phases, it would be better to introduce Pauli matrices:

$$\tau_1 = \begin{bmatrix} 0 & 1 \\ 1 & 0 \end{bmatrix}, \quad \tau_2 = \begin{bmatrix} 0 & -i \\ i & 0 \end{bmatrix}, \quad \tau_3 = \begin{bmatrix} 1 & 0 \\ 0 & -1 \end{bmatrix},$$

as well as the identity matrix $\tau_0 = \mathbb{I}_2$, which act on the coin space. The above three Pauli matrices are basic elements of $SU(2)$ matrices. They satisfy the following algebra:

$$\text{i)} \quad (\tau_i)^2 = \tau_0 \quad (i = 0, 1, 2, 3), \tag{E.3a}$$

$$\text{ii)} \quad \tau_i\tau_0 = \tau_0\tau_i = \tau_i \quad (i = 1, 2, 3), \tag{E.3b}$$

$$\text{iii)} \quad \tau_i\tau_j = -\tau_j\tau_i \quad (i, j = 1, 2, 3,\ i \neq j). \tag{E.3c}$$

By expanding the exponential function and using Eqs. (E.3a) and (E.3b), it is straight forward to derive the following relation:

$$e^{ia\tau_i} = \cos(a)\tau_0 + i\sin(a)\tau_i \quad (i = 0, 1, 2, 3), \tag{E.4}$$

where $a \in \mathbb{R}$.
We can express the shift and coin operators by Pauli matrices. The split-shift operators in Eqs. (E.2a) and (E.2b) are written as follows:

$$S_\pm \quad = \quad \frac{1}{2}\big[\,(|x\rangle\langle x| + |x\rangle\langle x \mp 1|)\,\tau_0 \pm (|x\rangle\langle x| - |x\rangle\langle x \mp 1|)\,\tau_3\big].$$

By using Eq. (E.4), the coin operator in Eq. (E.1) is written as

$$U_{\sigma_0,\theta} = R_{\sigma_0,\theta}\cdot\tau_3 = e^{-i\phi}\cdot R_{\sigma_0,\theta}\cdot e^{-i\chi\tau_3}, \quad \chi = -\phi = \pi/2, \tag{E.5a}$$

$$R_{\sigma_0,\theta} = \begin{bmatrix} \cos(\theta) & -e^{i\sigma_0}\sin(\theta) \\ e^{-i\sigma_0}\sin(\theta) & \cos(\theta) \end{bmatrix} = e^{-i\theta[\sin(\sigma_0)\tau_1 + \cos(\sigma_0)\tau_2]}. \tag{E.5b}$$

Therefore, the time-evolution operator can be written as follows:

$$U^{(s)} = SU_{\sigma_0,\theta} = e^{-i\phi}\cdot S_-\cdot S_+\cdot R_{\sigma_0,\theta}\cdot e^{-i\chi\tau_3}, \quad \chi = -\phi = \pi/2. \tag{E.6}$$

Hereafter, we examine the relevant symmetries for topological phases of the time-evolution operator in Eq. (E.6). First, we focus on identifying chiral symmetry Eq. (10) by applying the method developed in Refs. [4, 35]. We understand that Eq. (10) is satisfied when the time-evolution operator $U^{(s)}$ is decomposed as follows:

$$U^{(s)} = e^{-i\varepsilon_\Gamma} F\cdot\Gamma^{-1}F^{-1}\Gamma, \tag{E.7}$$

with the help of the relation $\Gamma = \Gamma^{-1}$. In order to confirm Eq. (E.7) for the time-evolution operator of the complete two-phase QW, we need to shift the origin of time by a half of the coin operator to fit into a *symmetry time frame* introduced in Ref. [4]. We also use the commutation relation between $S_\pm$ and $e^{-i\chi\tau_3}$, since both are described only by τ_0 and τ_3 components. Thereby, we obtain the single-step time-evolution operator in the symmetry time frame:

$$U^{(s)\prime} \quad = \quad e^{-i\phi}R_{\sigma_0,\theta/2}\cdot e^{-i(\chi/2)\tau_3}\cdot S_-\cdot S_+\cdot e^{-i(\chi/2)\tau_3}\cdot R_{\sigma_0,\theta/2}. \tag{E.8}$$

Note we use relations $R_{\sigma_0,\theta} = R_{\sigma_0,\theta/2}\cdot R_{\sigma_0,\theta/2}$ and $e^{-i\chi\tau_3} = e^{-i(\chi/2)\tau_3}\cdot e^{-i(\chi/2)\tau_3}$.
Comparing the global phase factors in Eq. (E.7) with Eq. (E.8), we identify $\varepsilon_\Gamma = \phi = -\pi/2$. Then, comparing the rest parts, we identify $F = R_{\sigma_0,\theta/2}\cdot e^{-i(\chi/2)\tau_3}\cdot S_-$ and chiral symmetry requires the condition:

$$\Gamma(S_+\cdot e^{-i(\chi/2)\tau_3}\cdot R_{\sigma_0,\theta/2})\Gamma^{-1} = (R_{\sigma_0,\theta/2}\cdot e^{-i(\chi/2)\tau_3}\cdot S_-)^{-1}.$$

Taking account of $(R_{\sigma_0,\theta})^{-1} = R_{\sigma_0,-\theta}$, chiral symmetry is established if the following conditions are satisfied:

$$\Gamma R_{\sigma_0,\theta}\Gamma^{-1} = R_{\sigma_0,-\theta}, \tag{E.9a}$$

$$\Gamma e^{-i(\chi/2)\tau_3}\cdot S_\pm\Gamma^{-1} = e^{+i(\chi/2)\tau_3}\cdot(S_\mp)^{-1}. \tag{E.9b}$$

When $\sigma_0 = 0$, the chiral symmetry operator $\Gamma = \sum_x |x\rangle\langle x|\otimes\tau_1$ satisfies the above conditions[35]. However, for the arbitrary value of σ_0, the above Γ does not satisfy Eq. (E.9a), while it does Eq. (E.9b). The point is $R_{\sigma_0,\theta}$ in Eq. (E.5b) contains the τ_1 component which commutes with the chiral symmetry operator Γ. This problem is solved by removing the τ_1 component by a unitary transformation before τ_1 acts, and then recovering it by another unitary transformation. In summary, $U^{(s)\prime}$ has chiral symmetry with the following chiral symmetry operator Γ;

$$\Gamma\, e^{i\varepsilon_\Gamma}U^{(s)\prime}\,\Gamma^{-1} = \left(e^{i\varepsilon_\Gamma}U^{(s)\prime}\right)^{-1}, \quad \text{with } \varepsilon_\Gamma = -\frac{\pi}{2}, \tag{E.10a}$$

$$\Gamma = \sum_x |x\rangle\langle x|\otimes V_{\sigma'}\,\tau_1\,V_{\sigma'}^{-1}, \quad V_{\sigma'} := e^{i(\sigma'/2)\tau_3}, \quad \sigma' = \sigma_0. \tag{E.10b}$$

Next, we focus on particle-hole symmetry Eq. (9). While the symmetry time frame is unnecessary to define particle-hole symmetry, we keep using the time-shifted time-evolution operator $U^{(s)\prime}$. Taking into account the fact that $V_{\sigma_0}^{-1} R_{\sigma_0,\theta} V_{\sigma_0} = R_{0,\theta}$ and $e^{-i\phi} e^{-i\chi\tau_3} = \sigma_z$ with $\chi = -\phi = \pi/2$ are expressed by real numbers, particle-hole symmetry of $U^{(s)\prime}$ is identified as follows:

$$
\begin{aligned}
&P\, e^{i\varepsilon_P} U^{(s)\prime}\, P^{-1} = e^{i\varepsilon_P} U^{(s)\prime}, \quad \text{with } \varepsilon_P = 0, \\
&P = \sum_x |x\rangle\langle x| \otimes V_{\sigma'}\, \tau_0 K\, V_{\sigma'}^{-1}, \quad \sigma' = \sigma_0
\end{aligned}
$$

Appendix F

Once chiral symmetry is identified, the topological number of the time-evolution operators $U^{(s)\prime}$ can be calculated from the Berry phase, or the winding number. In case of the presence of chiral symmetry, an important difference of topological phases of quantum walks from those of time-independent topological insulators is the existence of two topological numbers, ν_{ε_Γ} and $\nu_{\varepsilon_\Gamma+\pi}$, because of 2π periodicity of quasi-energy. According to the method to calculate the two topological numbers developed in Ref. [4], we prepare two time-evolution operators which have different symmetry time frames. Considering Eq. (E.7), we find the other time-evolution operator $U^{(s)} = e^{-i\varepsilon_\Gamma} \Gamma^{-1} F^{-1} \Gamma \cdot F$, in which the order of operators is inverted, also satisfies chiral symmetry Eq. (10). For explicitly, the other chiral symmetric time-evolution operator of the complete two-phase QW is expressed as

$$
U^{(s)\prime\prime} = e^{-i\phi} S_+ \cdot e^{-i(\chi/2)\tau_3} \cdot R_{\sigma_0,\theta/2} \cdot R_{\sigma_0,\theta/2} \cdot e^{-i(\chi/2)\tau_3} \cdot S_-, \quad \chi = -\phi = \pi/2.
$$

We also apply a unitary transformation into the two time-evolution operators so as to make calculations of the Berry phase simple. Hereafter, we treat the following two time-evolution operators under the unitary transformation:

$$
\begin{aligned}
\tilde{U}^{(s)\prime} &= V^{-1}\, U^{(s)\prime}\, V, \\
\tilde{U}^{(s)\prime\prime} &= V^{-1}\, U^{(s)\prime\prime}\, V, \\
V &= V_{\sigma'} e^{-i(\pi/4)\tau_2}, \quad \sigma' = \sigma_0.
\end{aligned}
$$

Since there are no position dependent parameters in $\tilde{U}^{(s)\prime}$ and $\tilde{U}^{(s)\prime\prime}$, the system has translation invariance, and then we consider the time-evolution operators $\tilde{U}^{(s)\prime}(k)$ and $\tilde{U}^{(s)\prime\prime}(k)$ in the momentum (wave-number) space representations by applying the Fourier transformation. The winding number ν and the Berry phase φ_B is calculated from the eigen function $\psi(k)$ of the time-evolution operators in the momentum space representation as

$$
\nu = \frac{\varphi_B}{\pi}, \quad \varphi_B = \frac{1}{i} \int_{-\pi}^{\pi} dk\, \psi^*(k) \frac{d}{dk} \psi(k).
$$

The time-evolution operator $\tilde{U}^{(s)\prime}$ in the momentum representation becomes

$$
\begin{aligned}
\tilde{U}^{(s)\prime}(k) &= \begin{bmatrix} c_k c_\theta & -r_k e^{i\phi'_k} \\ r_k e^{-i\phi'_k} & c_k c_\theta \end{bmatrix}, \\
r_k &= \sqrt{1 - c_k^2 c_\theta^2} \geq 0, \quad e^{i\phi'_k} = r_k^{-1}(c_k s_\theta + i s_k),
\end{aligned}
$$

with the shorthands

$$c_x := \cos(x), \quad s_x := \sin(x).$$

Note that we redefine $k - \chi$ as k since the shift of momentum by χ does not change the Berry phase. We also put $\phi = 0$ since the phase ϕ only shifts the origin of quasi-energy, which again does not change the Berry phase. The eigenvalues of $\tilde{U}^{(s)\prime}$ is

$$\lambda'_{\pm} = e^{\pm i\varepsilon} = c_k c_\theta \pm i r_k.$$

The corresponding eigenvectors are

$$\psi'_{\pm}(k) = \frac{1}{\sqrt{2}} \begin{pmatrix} \pm i e^{i\phi'_k} \\ 1 \end{pmatrix}$$

Then, the winding number ν' calculated from $\psi'_{\pm}(k)$ is given by

$$\begin{aligned} \nu' = &= \frac{1}{2\pi} \oint d\phi'_k \\ &= \begin{cases} +1 & \text{for } 0 < \theta < \pi \\ -1 & \text{for } -\pi < \theta < 0 \end{cases} \end{aligned} \tag{F.1}$$

In the same way, the time-evolution operator $\tilde{U}^{(s)\prime\prime}$ becomes

$$\tilde{U}^{(s)\prime\prime} = \begin{bmatrix} c_k c_\theta & -r_k e^{i\phi''_k} \\ r_k e^{-i\phi''_k} & c_k c_\theta \end{bmatrix},$$
$$e^{i\phi''_k} = r_k^{-1}(s_\theta + i s_k c_\theta).$$

Again, we redefine $k - \chi$ as k and put $\phi = 0$. The eigenvalue of $\tilde{U}^{(s)\prime\prime}$ is the same with $\lambda'_{\pm}$ of $\tilde{U}^{(s)\prime}$ and the corresponding eigenvectors are

$$\psi''_{\pm}(k) = \frac{1}{\sqrt{2}} \begin{pmatrix} \pm i e^{i\phi''_k} \\ 1 \end{pmatrix}$$

The winding number ν'' calculated from $\psi''_{\pm}(k)$ is given by

$$\begin{aligned} \nu'' &= \frac{1}{2\pi} \oint d\phi''_k \\ &= 0 \quad \text{for } -\pi < \theta < \pi. \end{aligned} \tag{F.2}$$

Ref. [4] derives that the topological numbers ν_0 and ν_π for quasi-energy 0 and π, respectively, are given by

$$\nu_0 = \frac{\nu'' + \nu'}{2}, \qquad \nu_\pi = \frac{\nu'' - \nu'}{2}. \tag{F.3}$$

Hence, by using Eqs. (F.1)-(F.3), we obtain the topological number ν_0 and ν_π for quasi-energy $\varepsilon = 0$ and π, respectively, as follows:

$$(\nu_0, \nu_\pi) = \begin{cases} (+1/2, -1/2) & 0 < \theta < \pi \\ (-1/2, +1/2) & -\pi < \theta < 0 \end{cases}$$

According to the bulk-edge correspondence, the number of edge states comes from the absolute value of the difference of topological numbers of the two adjacent spatial regions. This allows us to add a constant to all

topological numbers. Also, we need recover $\phi(=\varepsilon_\Gamma)$ to $-\pi/2$. Thereby, by adding $1/2$ into the all topological numbers and shifting the origin of quasi-energy by $-\pi/2$, we reach to the following result:

$$(\nu_{-\pi/2}, \nu_{+\pi/2}) = \begin{cases} (1,0) & 0 < \theta < \pi \\ (0,1) & -\pi < \theta < 0 \end{cases} \tag{F.4}$$

Finally, we apply the above result to the complete two-phase QW. First, we consider the topological numbers for the complete two-phase QW with the phase σ_+ in the region $x \geq 0$. By putting $\sigma_0 = \sigma' = \sigma_+$ of $R_{\sigma_0,\theta}$ and $V_{\sigma'}$, and fixing $\theta = \pi/4$, we obtain Eq. (15). Then, we focus on those for the complete two-phase QW with the phase σ_- in the region $x \leq -1$. In order to retain chiral symmetry of the whole of complete two-phase QW, we have to use the same chiral symmetry operator Γ. If we choose the phase $\sigma' = \sigma_+$ in $V_{\sigma'}$ in Eq. (E.10b), σ_- should be

$$\sigma_- = \sigma_+ + n\pi \quad (n \in \mathbb{Z}).$$

Taking account of the relation

$$V_{\sigma_+}^{-1} R_{\sigma_-,\theta} V_{\sigma_+} = V_{\sigma_+}^{-1} R_{\sigma_+ + n\pi,\theta} V_{\sigma_+} = R_{\sigma_+,(-1)^n\theta},$$

and Eq. (F.4), we obtain Eq. (17).